Smooth Diagnostic Expectations*

Francesco Bianchi Cosmin Ilut Hikaru Saijo
Johns Hopkins University Duke University UC Santa Cruz
CEPR and NBER NBER

May 22, 2024

Abstract

We introduce "smooth diagnosticity." Under smooth diagnosticity, agents overreact to new information defined as the difference between the current information set and a previous information set. Since new information typically changes not just the conditional mean, but also the conditional uncertainty, changes in uncertainty surrounding current and past beliefs affect the severity of the Diagnostic Expectations (DE) distortion. Smooth DE nests the baseline DE of Bordalo et al. (2018) and implies a joint and parsimonious micro-foundation for various properties of survey data: (1) overreaction of conditional mean to news, (2) stronger overreaction for weaker signals and longer forecast horizons, and (3) overconfidence in subjective uncertainty. We embed Smooth DE in an analytical RBC model. The model accounts for overreaction and overconfidence in surveys, as well as three salient properties of the business cycle: (1) asymmetry, (2) countercyclical micro volatility, and (3) countercyclical macro volatility.

JEL Codes: D91, E32, E71.

Keywords: Diagnostic expectations, uncertainty, learning, overreaction, overconfidence

^{*}Emails: francesco.bianchi@jhu.edu, cosmin.ilut@duke.edu, and hsaijo@ucsc.edu. We thank Joel Flynn, Spencer Kwon, Chen Lian, Karthik Sastry, Andrei Shleifer, Stephen Terry, Alonso Villacorta, as well as conference participants at the ASSA 2024 Annual Meeting. Saijo gratefully acknowledges the financial support of the Grants-in-Aid for Scientific Research (JP21H04397) from the Japan Society for the Promotion of Science.

1 Introduction

There has been a growing interest in psychological foundations that enrich models of belief formation in economics. A prominent example is the "representative heuristic" of Kahneman and Tversky (1972), which serves as the underpinning of a recent and expanding literature on the paradigm of Diagnostic Expectations (DE). According to this heuristic, when new information arrives, as measured with respect to a reference distribution based on past data, memory selectively recalls more vividly past events that are more associated with, or representative of, that current news. Models of DE formalize the details on how memory retrieval distorts the subjective probability of uncertain events away from its objective, "kernel of truth," frequency (see Bordalo et al. (2022) for an overview).

One immediate manifestation of the kernel of truth logic is that when the new information completely eliminates uncertainty over the variable to be forecast, there is objectively no room for memory to distort conditional judgements (Gennaioli and Shleifer (2010)). While in existing DE models this logic holds in its extreme version of no conditional uncertainty, the literature has so far not captured a "smoothed" version of the same intuition, namely that the severity of the DE distortion might depend on conditional uncertainty.

Smooth Diagnostic Expectations. We contribute to the theoretical development of the DE paradigm by providing a framework that captures such "smooth diagnosticity". Under the Smooth Diagnostic Expectations (Smooth DE) framework, agents overreact to new information defined as the difference between the current information set and a previous information set. Since new information typically changes not just the conditional mean, but also the conditional uncertainty, changes in uncertainty surrounding current and past beliefs affect the extent of the DE distortion. This is a minimal, but conceptually important change to the baseline DE paradigm developed by Bordalo et al. (2018) (BGS) and it aligns well with the original "representative heuristic" of Kahneman and Tversky (1972). In the BGS formulation, the reference distribution is centered on the conditional mean under the true density formed at some given past time, but shares the same uncertainty as the true distribution conditional on current information. Instead, since we condition exclusively on the past information set, the reference distribution reflects the level of uncertainty at that past time in which expectations were formed, as opposed to the current level of uncertainty.

When the current and reference distributions are Normal, the baseline BGS formulation delivers a distorted distribution that is also Normal, but in which only the mean is affected by DE. In comparison, under Smooth DE we uncover two key novel properties of the distorted distribution. First, the severity of the Smooth DE distortion decreases as the current level of uncertainty decreases compared to past uncertainty. Put differently, we obtain a smooth

version of the logic expressed by Gennaioli and Shleifer (2010), as now an agent is less prone to overreact to the new information the more precise the current information is with respect to past information. In the limit, as uncertainty is fully resolved by the new information, the distortion vanishes, as in the baseline DE. However, with Smooth DE, the extent of the distortion varies smoothly as current uncertainty increases with respect to past uncertainty, while the baseline DE features a discontinuity once current uncertainty goes to zero.

Second, Smooth DE delivers a disconnect between the *objective* and *subjective* level of uncertainty. This is because under Smooth DE, not only the mean, but also the variance of the DE distribution is distorted. When agents experience a reduction in uncertainty with respect to the reference distribution, agents over-state the precision of their forecasts, leading to *overconfidence*. In other words, in that case the DE distribution features a variance lower than under RE. Given that typically events close in the future are easier to predict than events far into the future, agents' beliefs will typically feature such overconfidence. However, the Smooth DE paradigm can also accommodate *underconfidence* following an increase in uncertainty, like in response to an uncertainty shock (Bloom (2009)).

We incorporate Smooth DE within a signal extraction environment, by extending the Diagnostic Kalman filter of Bordalo et al. (2019). This application is particularly interesting because by allowing for imperfect information, we can study how the degree of overreaction and confidence varies with the degree of uncertainty due to learning about the underlying state. Under the Smooth Diagnostic Kalman filter, the posterior mean features overreaction to news, as in the original Diagnostic Kalman filter. However, under Smooth DE the degree of overreaction depends on the level of current uncertainty (posterior variance) about the hidden state relative to past uncertainty (prior variance). Furthermore, compared to the Bayesian forecast, the conditional forecast implied by the Smooth Diagnostic Kalman Filter systematically exhibits not only (a) overreaction of the conditional mean, but also (b) overconfidence: The subjective uncertainty is lower than the corresponding Bayesian uncertainty.

A parsimonious micro-foundation for survey evidence. As the traditional DE, Smooth DE is characterized by a primitive stochastic environment and two parameters controlling (i) the severity of the distortion, $\theta > 0$, and (ii) the lag of the reference distribution, $J \ge 1$. Thus, Smooth DE makes use of no additional degree of freedom. Instead, by allowing the reference distribution to be based only on the information set available at some given past time, the kernel of truth logic endogenously generates predictions for the effective distortion. Under Smooth DE, the primitive parameter $\theta > 0$ measures the severity of the DE distortion for a given level of relative uncertainty, while the effective severity changes with the relative uncertainty. These disciplined predictions allow Smooth DE to offer a parsimonious

micro-foundation for a wide range of stylized facts.

The novel property that the effective overreaction to news is stronger when relative uncertainty is higher helps to account for two sets of stylized survey facts. First, overreaction increases with the horizon of the survey forecast (see for example Bordalo et al. (2019), d'Arienzo (2020), Bordalo et al. (2020), Augenblick et al. (2021), and Bordalo et al. (2023)). Here we start by noting that for standard stationary processes the same piece of information is less informative about horizons further in the future. Critically, under Smooth DE this relatively smaller reduction in conditional uncertainty leads to a relatively stronger overreaction to news for longer horizons forecasts, consistent with the stylized findings.

Second, Augenblick et al. (2021) document that compared to Bayesian forecasts, decision-makers overreact to weaker signals while underreacting to stronger signals. To connect to these findings, we build into our proposed Smooth Diagnostic Kalman Filter a simple form of subjective attention noise perceived by the agent, which in isolation is a force towards underreaction compared to the econometrician's forecast. We show how the overreaction produced by the representativeness force behind Smooth DE can be relatively stronger than the cognitive noise effect for weaker signals, but not for stronger signals, leading to measured overreaction for the former, but underreaction for the latter. The key mechanism is again that, under Smooth DE, stronger signals reduce agent's conditional uncertainty more than weaker signals, dampening the impact of representativeness on forecasts.

The property that Smooth DE implies a disconnect between subjective and measured uncertainty makes the proposed framework relevant for a separate literature on overconfidence. Recent work documents that in survey data firms (i) overreact to news and (ii) are overconfident in their subjective forecasts (see, among others, Barrero (2022), Born et al. (2022), and the reviews in Altig et al. (2020) and Born et al. (2022)). While the baseline DE model can account for overreaction, it is silent on overconfidence. Smooth DE can instead account for both these seemingly separate properties since it distorts both the mean and the variance of agents' expectations in a way to typically generate both overreaction and overconfidence.

More broadly, the overreaction and overconfidence properties have been typically studied in the literature as two distinct behavioral departures from full rationality (see Barberis (2018) for an overview). While overreaction has been typically the focus on the standard DE literature, a separate literature (including for example De Bondt and Thaler (1995) and Daniel et al. (1998, 2001)) is motivated by extensive psychological evidence for overconfidence and argues that models based on this behavioral property are promising in accounting for asset market puzzles. Our results elucidate that Smooth DE can offer a *joint microfoundation*, based on the representativeness heuristic, of these two-widely documented and

studied departures from standard Bayesian updating.

Business cycle implications. We leverage our theoretical insights to study a parsimonious business cycle model with time-varying uncertainty to illustrate how state-dependent over-reactions from Smooth DE generate important cyclical implications. We consider an island economy subject to economy-wide and island-specific TFP shocks. Following Bloom et al. (2018), we assume that the island-specific TFP shocks are subject to time-varying volatility that is negatively correlated with economy-wide TFP innovations. We show that this parsimonious model can account for Barrero (2022)'s survey evidence on overreaction and overconfidence, as well as three key empirical properties of the business cycle: (1) asymmetry (recessions are deeper than expansions), (2) countercyclical micro volatility (cross-sectional variances of microeconomic variables rise in recessions), and (3) countercyclical macro volatility (time-series variances of macroeconomic variables rise in recessions).

First, consider the asymmetry property. A negative economy-wide TFP shock generates higher uncertainty about the island-specific TFP shocks. Hence, agents overreact to the economy-wide TFP shock more than usual, leading to a sharper fall in hours, consumption, and output. In contrast, a positive TFP shock reduces agents' uncertainty, and the rise in economic activity is mild. Second, consider countercyclical micro volatility. In recessions, agents face higher uncertainty, so they overreact to the island-specific TFP and as a result, the cross-sectional variances of island-level hours, output, and consumption increase. Conversely, during expansions, agents' overreactions are milder, and hence the cross-sectional dispersion decreases. Third, consider countercyclical macro volatility. The state-dependent overreaction implies that in recessions, economic activity responds strongly to an economy-wide shock to TFP, while in expansions the responses are more muted. As a result, the aggregate volatility rises in recessions even when there is no change in the volatility of economy-wide shocks. These mechanisms highlight that the micro-level uncertainty and macroeconomic volatility are tightly linked through the agent's state-dependent overreaction. As a result, a novel policy implication emerges: a redistributive policy that reduces idiosyncratic uncertainty could be beneficial for macroeconomic stabilization because it dampens this state-dependent overreaction.

Outline. In Section 2, we derive the Smooth DE density and discuss its properties. In Section 3, we show how Smooth DE can serve as a joint and parsimonious micro-foundation for various properties of survey data. In Section 4, we showcase the macroeconomic implications

¹These properties have been extensively documented in the literature. For instance, Neftci (1984), Hamilton (1989), Sichel (1993), McKay and Reis (2008), and Morley and Piger (2012) show macroeconomic asymmetries using various econometric approaches. Bloom (2009), Fernández-Villaverde et al. (2011), Ilut et al. (2018), Jurado et al. (2015), Basu and Bundick (2017), and Bloom et al. (2018) document that volatility or uncertainty rise in recessions at the micro and macro levels.

of Smooth DE using an analytical RBC model with time-varying uncertainty.

2 The Smooth Diagnostic Expectations density

Our starting motivation is the Gennaioli and Shleifer (2010) definition of representativeness of a given trait \hat{x} for a group G as

$$\frac{f(\widehat{x}|G)}{f(\widehat{x}|-G)}\tag{1}$$

where -G is the reference group, and $f(\widehat{x}|G)$ and $f(\widehat{x}|G)$ are true distributions. In building this definition, Gennaioli and Shleifer (2010) explain in detail how representativeness can be intuitively understood as the tendency to overweight representative traits, arising due to limited memory and the fact that representative traits are easier to recall.

2.1 Discrete distributions

To understand how we connect to the original concept of representativeness in a time series dimension, it is useful to first consider a series of simple examples. These examples are based on discrete distributions and are meant to illustrate how in rich settings, the whole distribution contributes to pin down the level of overreaction to new information. Along the way, we will also show how implicitly the support of the distribution and the level of detail in the information and reference group contribute to shaping the level of overreaction. This will allow us to draw an explicit connection between the representativeness heuristic and Smooth DE as developed below.

Two states. Consider a simple example in which \hat{x} is the hair color of a person. This can assume only two values, "red" or "non-red/other", which we denote as R and NR, respectively. The numbers here are chosen to illustrate a series of key features of representativeness and are not necessarily reflecting the actual incidence of the hair color red in the world population. In this first example, "-G" coincides with the information set available to an agent before learning the nationality of a person. "G" is the information set once the nationality is revealed. The agent subject to the representativeness heuristic distorts the true probabilities by the following weights, where:

$$\text{Weight} \left(\widehat{x} = i \right) = \left(\frac{\text{Posterior}(\widehat{x} = i)}{\text{Prior}(\widehat{x} = i)} \right)^{\theta} \frac{1}{Z}, \quad Z = \sum_{i} \text{Posterior}(\widehat{x} = i) \left(\frac{\text{Posterior}(\widehat{x} = i)}{\text{Prior}(\widehat{x} = i)} \right)^{\theta},$$

where i = R, NR. Thus, the distorted probability of hair color being red is given by

$$P^{\theta}(\widehat{x} = R) = \text{Posterior}(\widehat{x} = R) \text{Weight}(\widehat{x} = R)$$
.

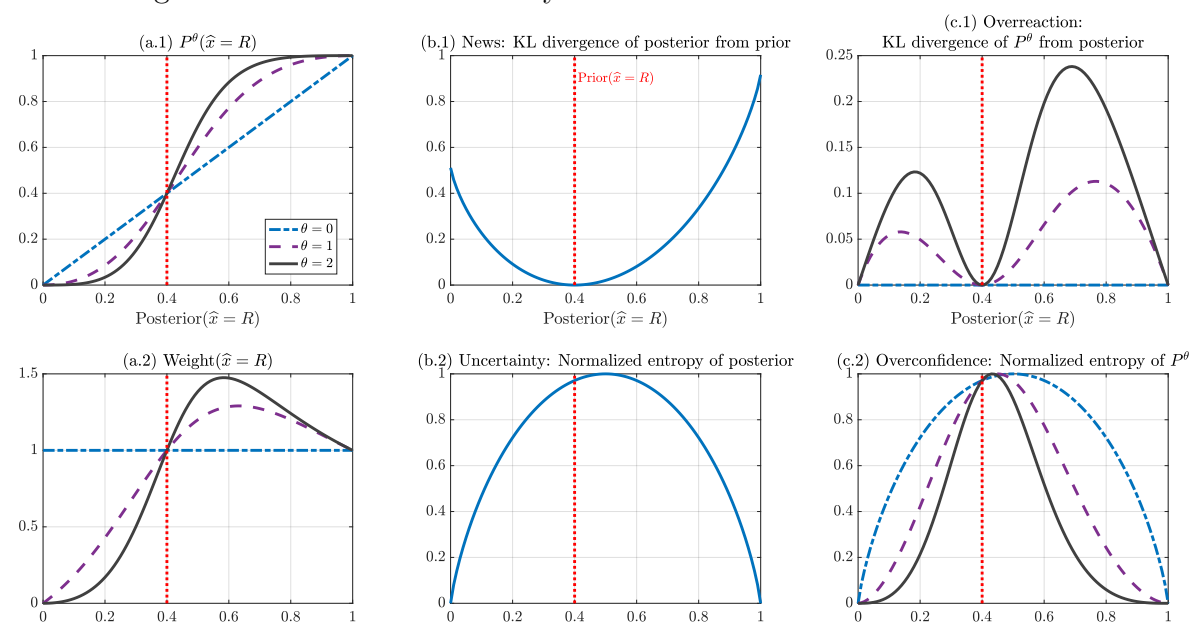


Figure 1: News and uncertainty in a two-states discrete distribution

Notes: The figure displays how, as we vary the posterior probability of a red hair color $(\hat{x} = R)$, the following objects change: (a.1) the distorted probability of red hair, (a.2) the distorting weight on the red hair probability, (b.1) the news component, measured using the KL divergence of the posterior distribution from the prior distribution, (b.2) the uncertainty component, measured using the normalized entropy of the posterior distribution, (c.1) the overall overreaction, measured using the KL divergence of the distorted probability distribution from the posterior distribution, and (c.2) the normalized entropy of the distorted probability distribution. We fix the prior probability of a red hair color at $Prior(\hat{x} = R) = 0.4$.

Posterior($\hat{x} = R$)

Posterior($\hat{x} = R$)

For instance, imagine "G = Irish." In this case, Posterior($\hat{x} = i$) = $P(\hat{x} = i|Irish)$ and $Prior(\hat{x} = i) = P(\hat{x} = i|Unknown)$. The new information implies an objective increase in the probability of the hair color being red. The red color becomes more representative of the Irish population, and, as a result, the agent subject to the representativeness heuristic distorts the true probabilities of a red hair color by

Weight
$$(\widehat{x} = R) = \left(\frac{P(\widehat{x} = R|Irish)}{P(\widehat{x} = R|Unknown)}\right)^{\theta} \frac{1}{Z}.$$

We are interested in how the distorted probability distribution and its distance (appropriately defined) from the true posterior distribution depend on the underlying probability distributions. In Figure 1 (a.1), we plot the distorted probability $P^{\theta}(\hat{x} = R)$ for different values of Posterior($\hat{x} = R$). The prior probability is set at Prior($\hat{x} = R$) = 0.4. We also plot $P^{\theta}(\hat{x} = R)$ for different diagnosticity parameter values $\theta = 0, 1, 2$. $\theta = 0$ corresponds to

the RE case where $P^{\theta}(\widehat{x}=R)=\text{Posterior}(\widehat{x}=R)$. When the posterior is lower than the prior, the distorted probability is lower than the posterior. Conversely when the posterior is higher than the prior, the distorted probability is higher than the posterior. The magnitude of the difference between the distorted probability and the posterior is increasing in θ . Finally, this difference is hump-shaped. The difference between the distorted and posterior probabilities is the largest for intermediate values between the prior of 0.4 and the lower and upper bounds (0 and 1). Figure 1 (a.2) reports how the distorting weight, Weight $(\widehat{x}=R)$, is non-monotonic in the posterior: the weight is increasing from Posterior $(\widehat{x}=R)=0$ to some intermediate value between $\text{Prior}(\widehat{x}=R)=0.4$ and then start decreasing. Mathematically this is because the constant of integration Z in the distorting weight becomes larger as posterior probability of red hair approaches 1. Intuitively, as the posterior becomes more certain towards one type, the room for distortion becomes smaller as the total probability has to sum to 1. This is the first observation indicating not only the revision of posterior from the prior, but also uncertainty, matter for the representativeness distortion.

In panel (b.1), we measure the size of the news component: the size of the revision of the posterior distribution from the prior distribution by computing the Kullback–Leibler (KL) divergence of the two distributions:

$$KL(\operatorname{Posterior}||\operatorname{Prior}) = \sum_{i} \operatorname{Posterior}(\widehat{x} = i) \ln \left(\frac{\operatorname{Posterior}(\widehat{x} = i)}{\operatorname{Prior}(\widehat{x} = i)} \right).$$

The KL divergence is U-shaped, with KL = 0 when the posterior distribution is equal to the prior distribution. Panel (b.2) plots normalized entropy, which is our measure of posterior uncertainty. The normalized entropy of posterior distribution is given by

$$\Omega(\operatorname{Posterior}) = -\frac{\sum_{i} \operatorname{Posterior}(\widehat{x} = i) \ln \operatorname{Posterior}(\widehat{x} = i)}{\ln(2)},$$

where the denominator ensures the entropy is between 0 and 1. The entropy shows an inverted U-shape and peaks when the posterior is 50:50. Panel (c.1) shows the degree of overreaction, as measured by the KL divergence between the distorted distribution and the posterior distribution: $KL(P^{\theta}||\text{Posterior})$. The degree of overreaction again shows two humps: a smaller one that peaks at the intermediate value between 0 and $\text{Prior}(\hat{x} = R) = 0.4$ and a larger one that peaks at the intermediate value between $\text{Prior}(\hat{x} = R) = 0.4$ and 1. The two humps are the result of the interaction between news and uncertainty effects, which both magnify overreaction, but display different patterns (U- and inverted U-shape). The sizes of the two humps are different because the trough of the news component and the model point of the uncertainty effect do not coincide. Finally, panel (c.2) considers the

normalized entropy of the distorted distribution P^{θ} . Lower entropy relative to the posterior distribution means overconfidence; the agent is too certain about the hair color compared to the true distribution. Indeed, the entropy of the distorted distribution exhibits bell-shapes, rather than an inverted U-shape like for the posterior, indicating overconfidence except for the posterior probability around 0.5. There, since the posterior entropy is larger than the entropy at the prior of 0.4, the agent exhibits underconfidence. The degree of overconfidence is more severe for the posterior on the right tail (Posterior($\hat{x} = R$) > 0.6) than the posterior on the left tail (Posterior($\hat{x} = R$) < 0.4). This is because the news effect is larger for the posterior on the right tail than that on the left tail. To summarize the discussion on Figure 1, the two-states example shows news and uncertainty both interact in a rich manner to determine the overall degree of overreaction and overreaction.

Three states. Consider instead of two hair colors, suppose there are "red", "blond", and "dark" hair colors, denoted by R, B, and D, respectively. We consider a prior equally split between R and B so that $Prior(\hat{x} = R) = Prior(\hat{x} = B) = 0.2$ and $Prior(\hat{x} = D) = 0.6$. This three-states example is instructive because posterior probabilities of R and B jointly determine the news and uncertainty component, thus underscoring the importance of the probability distribution shaping the degree of overreaction. In Figure 2, we use contour plots to examine how news and uncertainty affect the overall overreaction as we vary Posterior $(\hat{x} = R)$ and Posterior($\hat{x} = B$) when $\theta = 2$. To ease interpretation, we mark the coordinates corresponding to the prior with white pluses, and the coordinates representing equal probabilities for all three outcomes, $P(\hat{x} = R) = P(\hat{x} = B) = P(\hat{x} = D) = 1/3$, with red diamonds. Panels (a.1) and (a.2) report the distorted probability and the weight associated with a red hair color. As in the two-states example, the distorted probabilities overreact to the revision in the red hair probability from prior to posterior. The distorting weight of the red probability peaks when Posterior($\hat{x} = R$) takes an intermediate value between 0.2 and 1 and Posterior($\hat{x} = B$) takes an intermediate value between 0 and 0.2. Similarly, Panel (b.1) and (b.2) report the distorting probability and the weight associated with a blond hair color. Panel (c.1) displays the news component, measured as the KL divergence of the posterior distribution from the prior distribution. The news component increases as the posterior distribution moves away from the prior and peaks when either of the hair color outcomes reaches certainty (Posterior($\hat{x} = R$) = 1 or Posterior($\hat{x} = B$) = 1). The uncertainty component, reported in panel (c.2) peaks when the posterior distribution assigns equal probabilities for all three outcomes. Panel (d.1) reports the KL divergence from the distorted probability distribution to the posterior distribution. The overreaction displays twin peaks resembling the double humps displayed in the two-states example. Note, however, that in the current three-states example how the posterior probabilities are split matters for the overreaction.

Indeed, the overreaction is mild as we increase both the posterior probabilities of red and blond hairs simultaneously in equal proportions. Finally, panel (d.2) reports the normalized entropy of the distorted distribution. Compared to the entropy of the posterior, the entropy of the distorted distribution is smaller in most regions, indicating overconfidence (except for the neighborhood of the prior and the coordinate representing equal probabilities for all three outcomes). The overconfidence is most severe around the three corners of the triangle, when the posterior puts most probability weights on one hair color. Intuitively, as one specific hair color becomes more representative, the agent overestimates the probability of that hair color and becomes too certain. As in the two-states example, this three-states example thus underscores a nuanced but tight connection between news/uncertainty effects and overreaction/overconfidence.

2.2 Representativeness and information sets

In order to model the representativeness heuristic into time-series, we mirror the logic of equation (1), and interpret groups as different information sets. In particular, we define the representativeness of a random event \hat{x}_{t+h} for some horizon $h \geq 0$ periods in the future as

$$\frac{f\left(\widehat{x}_{t+h}|\mathcal{I}_{t}\right)}{f\left(\widehat{x}_{t+h}|\mathcal{I}_{t}^{ref}\right)}$$

where $f(\widehat{x}_{t+h}|\mathcal{I})$ is the true density given some arbitrary information set \mathcal{I} . With respect to the approach proposed by Gennaioli and Shleifer (2010) in equation (1), the current group G is represented by the current information set \mathcal{I}_t , and the reference group -G corresponds to a reference information set $\mathcal{I}_t^{ref} \subseteq \mathcal{I}_t$. The latter thus implicitly defines the current representativeness of an event.

Using this definition of the representativeness of an event, we then build on the DE formulation introduced in BGS to construct a conditional density $f^{\theta}(\widehat{x}_{t+h}|\mathcal{I}_t)$ distorted by representativeness, as

$$f^{\theta}\left(\widehat{x}_{t+h}|\mathcal{I}_{t}\right) = f\left(\widehat{x}_{t+h}|\mathcal{I}_{t}\right) \left[\frac{f\left(\widehat{x}_{t+h}|\mathcal{I}_{t}\right)}{f\left(\widehat{x}_{t+h}|\mathcal{I}_{t}^{ref}\right)}\right]^{\theta} \frac{1}{Z}$$
(2)

Here Z is a constant of integration and the parameter $\theta \geq 0$ measures the severity of the distortion. When $\theta = 0$, the agent's memory retrieval is perfect and beliefs collapse to the standard frictionless model. When $\theta > 0$, memory is limited and the agent's judgments are shaped by representativeness.

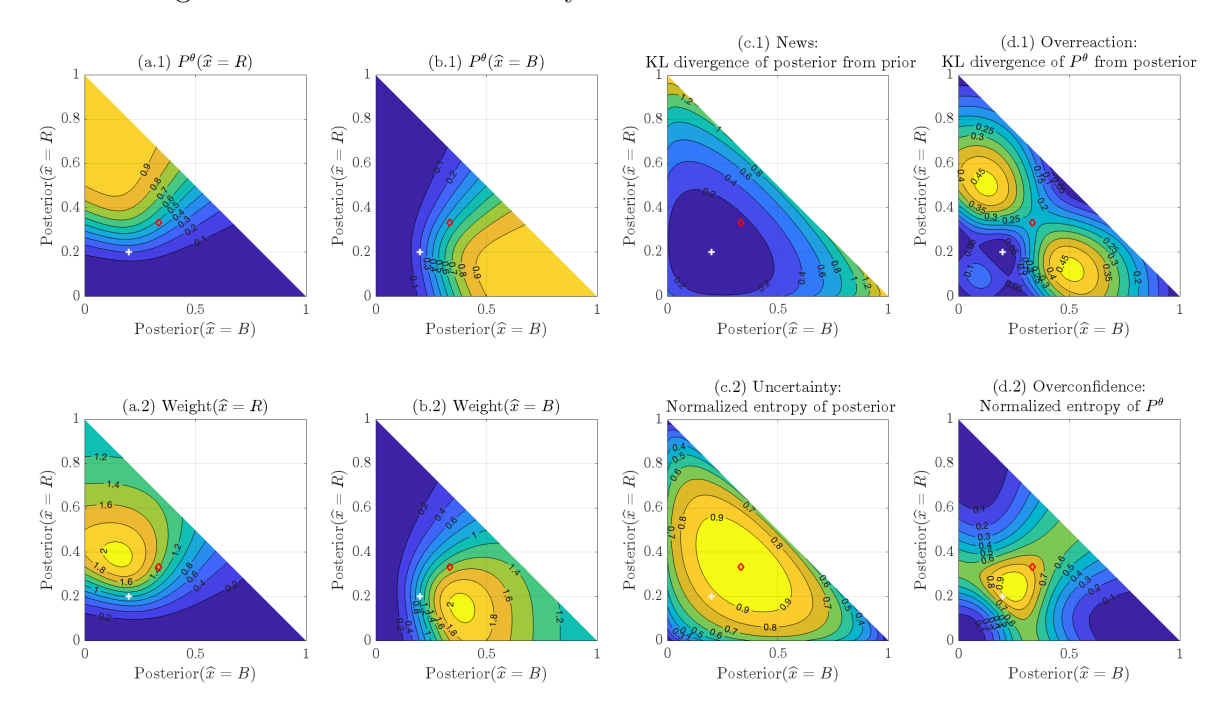


Figure 2: News and uncertainty in a three-states discrete distribution

Notes: The figure displays how, as we vary the posterior probability of red and blond hair colors ($\hat{x} = R$ and $\hat{x} = B$), the following objects change: (a.1) the distorted probability of red hair, (a.2) the distorting weight on the red hair probability, (b.1) the distorted probability of blond hair, (b.2) the distorting weight on the blond hair probability, (c.1) the news component, measured using the KL divergence of the posterior distribution from the prior distribution, (c.2) the uncertainty component, measured using the normalized entropy of the posterior distribution, (d.1) the overall overreaction, measured using the KL divergence of the distorted probability distribution from the posterior distribution, and (d.2) the normalized entropy of the distorted probability distribution. We mark the coordinates corresponding to the prior with white pluses, and the coordinates representing equal probabilities for all three outcomes with red diamonds.

Our bridge between the representativeness heuristic of Kahneman and Tversky (1972) and the time-series domain is then to define the reference information set as follows:

Assumption 1 Assume that the reference information set is the whole information set available $J \geq 1$ periods ago: $\mathcal{I}_t^{ref} = \mathcal{I}_{t-J}$.

Normal densities. To illustrate the specific and rich implications of this approach we follow BGS and focus on normal densities. As it will soon become clear, this leads to significant gains in tractability and in the range of possible applications. This is because when the true density is Normal, expression (2) delivers a closed form solution. In particular,

let the true densities conditional on the current and past information sets be:

$$f\left(\widehat{x}_{t+h}|\mathcal{I}_{t}\right) = \mathcal{N}\left(\widehat{x}_{t+h}; \mu_{t+h|t}, \sigma_{t+h|t}^{2}\right)$$

$$f\left(\widehat{x}_{t+h}|\mathcal{I}_{t-J}\right) = \mathcal{N}\left(\widehat{x}_{t+h}; \mu_{t+h|t-J}, \sigma_{t+h|t-J}^2\right)$$

Given Assumption 1, the reference group pinning down the current representativeness of the event \widehat{x}_{t+h} is then simply given by

$$f\left(\widehat{x}_{t+h}|\mathcal{I}_{t-J}^{\text{ref}}\right) = \mathcal{N}\left(\widehat{x}_{t+h}; \mu_{t+h|t-J}, \sigma_{t+h|t-J}^{2}\right). \tag{3}$$

2.3 Smooth DE

Under the proposed reference group given by equation (3), we obtain a closed form solution in Proposition 1 below for the distorted density, which we refer to as *Smooth Diagnostic Expectations*, or in a more abbreviated form as Smooth DE.

Proposition 1 (Smooth DE). Consider the reference group given by density in equation (3). Denote the ratio of variances for the current and reference groups as

$$R_{t+h|t,t-J} \equiv \sigma_{t+h|t}^2 / \sigma_{t+h|t-J}^2 \tag{4}$$

If $R_{t+h|t,t-J} < (1+\theta)/\theta$, the Smooth DE density $f^{\theta}(\widehat{x}_{t+h})$ in equation (2) is Normal with conditional mean

$$\mathbb{E}_{t}^{\theta}(x_{t+h}) = \mu_{t+h|t} + \theta \frac{R_{t+h|t,t-J}}{1 + \theta \left(1 - R_{t+h|t,t-J}\right)} \left(\mu_{t+h|t} - \mu_{t+h|t-J}\right)$$
 (5)

and conditional variance

$$\mathbb{V}_{t}^{\theta}\left(x_{t+h}\right) = \frac{\sigma_{t+h|t}^{2}}{1 + \theta\left(1 - R_{t+h|t,t-J}\right)} \tag{6}$$

Proof. See Appendix.

The condition $R_{t+h|t,t-J} < (1+\theta)/\theta$ guarantees that the variance of the resulting distorted Normal distribution is finite and positive. As the ratio of conditional variances between the current and reference distribution approaches this limiting value, the variance of the Smooth DE distribution approaches infinity and the corresponding Normal distribution approaches a degenerate, flat distribution. Thus, the condition requires that the current uncertainty with respect to a future event $(\sigma_{t+h|t}^2)$ is not too high with respect to the past

uncertainty about the same event $(\sigma_{t+h|t-J}^2)$. The condition typically holds in stationary environments with homoskedastic innovations in which events closer into the future are easier to predict than events far into the future. However, the condition also allows for the possibility of an increase in uncertainty, for example as a result of heteroskedasticity, as long as the increase is not too large with respect to the DE distortion.²

2.4 Standard DE

Under Normality, the assumption over the reference density in the denominator of equation (2) implies that the Smooth DE framework differs from the original BGS formulation with respect to the variance of the reference distribution. In BGS, the reference density uses the mean conditional on the information set J periods ago, but shares the same conditional uncertainty $\sigma_{t+h|t}$ as the true density $f(\widehat{x}_{t+h})$ conditional on the current information set:

Assumption 2 (BGS assumption) Assume that the density for the representative group is

$$f\left(\widehat{x}_{t+h}|\mathcal{I}_{t}^{ref}\right) = \mathcal{N}\left(\widehat{x}_{t+h}; \mu_{t+h|t-J}, \sigma_{t+h|t}^{2}\right)$$

$$\tag{7}$$

This BGS assumption delivers the following closed form standard DE density:

Proposition 2 (BGS implementation for DE). Consider the BGS assumption that the reference density is given by equation (7). When $\sigma_{t+h|t}^2 > 0$, the resulting DE density $f^{\theta}(\widehat{x}_{t+h})$ defined by equation (2) has a Normal distribution with mean:

$$\mathbb{E}_{t}^{\theta}(x_{t+h}) = \mu_{t+h|t} + \theta \left[\mu_{t+h|t} - \mu_{t+h|t-J} \right]. \tag{8}$$

and variance:

$$\mathbb{V}_t^{\theta}\left(x_{t+h}\right) = \sigma_{t+h|t}^2. \tag{9}$$

When $\sigma_{t+h|t}^2 = 0$, the DE conditional mean $\mathbb{E}_t^{\theta}(x_{t+h})$ collapses to $\mu_{t+h|t}$.

Proof. See Bordalo et al. (2018). ■

2.5 Novel properties and comparison with standard DE

Smooth DE is characterized by three important properties, which we will connect to stylized survey facts in Section 3. To understand these properties and the differences with the

²In Appendix B we discuss an approach that deals with this threshold condition by implementing an upper bound on the Smooth DE overreaction in the conditional mean. The approach guarantees that both the mean and variance distortions remain finite and non-decreasing as the ratio $R_{t+h|t,t-J}$ goes to infinity.

standard DE, it is helpful to define the effective overreaction of the conditional mean to news in equation (5) as

$$\widetilde{\theta}_{t,t-J} \equiv \theta \frac{R_{t+h|t,t-J}}{1+\theta \left(1 - R_{t+h|t,t-J}\right)}.$$
(10)

Corollary 1 Assume the presence of residual uncertainty with respect to a future event: $\sigma_{t+h|t}^2 > 0$. Compared to the RE forecast $(\theta = 0)$, the conditional forecast under Smooth DE $(\theta > 0)$, characterized in Proposition 1, exhibits

1. overreaction of the conditional mean to new information, since

$$\widetilde{\theta}_{t,t-J} > 0$$
 (11)

2. an effective overreaction of the conditional mean to new information that is monotonically increasing in the ratio $R_{t+h|t,t-J}$ between current and past uncertainty

$$\frac{\partial \widetilde{\theta}_{t,t-J}}{\partial R_{t+h|t,t-J}} > 0 \tag{12}$$

3. overconfidence when $R_{t+h|t,t-J} < 1$, since then by equation (6)

$$\mathbb{V}_{t}^{\theta}\left(x_{t+h}\right) < \sigma_{t+h|t}^{2} \tag{13}$$

or underconfidence when $R_{t+h|t,t-J} > 1$, since then by equation (6)

$$\mathbb{V}_{t}^{\theta}\left(x_{t+h}\right) > \sigma_{t+h|t}^{2}.\tag{14}$$

Novel properties. Under Smooth DE, we emphasize two types of novel properties corresponding to the distorted conditional moments in Proposition 1 and their properties emphasized in Corollary 1.

First, by equation (12), the severity of the mean distortion increases as the ratio $R_{t+h|t,t-J}$ of today's uncertainty to past uncertainty increases. Smooth DE thus micro-founds an inverse smooth link between overreaction of conditional mean to news and the (objective) informativeness of the new information compared to the reference distribution. The latter is captured by the ratio $R_{t+h|t,t-J}$: the more the new information reduces uncertainty $\sigma_{t+h|t}^2$ (compared to $\sigma_{t+h|t-J}^2$) the lower is the role of memory in distorting probability judgements, and thus the lower is the effective overreaction to news. Conversely, everything else equal, the larger today's uncertainty, the larger the observed Smooth DE distortion. As we will argue later in Section 3, this relationship between the conditional overreaction and the

change in conditional uncertainty helps Smooth DE to produce forecast implications that are consistent with a range of stylized facts documented by the survey literature. More broadly, even if the parameter θ controlling the severity of the Smooth DE distortion does not change, the observed deviations from rational expectations (RE) will change in response to changes in policymakers' behavior or perceived shifts in the size of the shocks. In this sense, the parameter θ has a structural interpretation, robust to the Lucas (1976) critique.

Second, Smooth DE has important implications for the level of subjective confidence that agents show with respect to their expectations. As summarized in Corollary 1, if agents experience a reduction of uncertainty with respect to the reference distribution, so that $R_{t+h|t,t-J} < 1$, Smooth DE implies a new property with respect to the original BGS formulation, namely overconfidence, i.e. agents overstate the precision of their expectations. Under this scenario, independently of the direction and size of the mean distortion, agents are overconfident about the precision of their expectations. If agents do not experience a change in uncertainty, $R_{t+h|t,t-J} = 1$, like in the BGS formulation, we do not observe a change in confidence with respect to RE. Finally, if agents experience an increase in uncertainty, so that $R_{t+h|t,t-J} > 1$, they will be less confident than the RE agents.

Nesting the original BGS formulation of DE. Our approach recovers the standard BGS formulation in two cases. First, in the limit case of no conditional uncertainty. In particular, note that in both approaches, with $\theta > 0$, there is a distortion if and only if the conditional variance $\sigma_{t+h|t}^2 > 0$. Intuitively, when $\sigma_{t+h|t}^2 = 0$, the conditional likelihood of observing any other scenario for x_{t+h} than the one the agent is now fully informed on (given that there is no positive uncertainty) has become equal to zero. As noted by Gennaioli and Shleifer (2010), the lack of such conditional (or "residual") uncertainty leaves no room for memory to distort conditional forecasts. In fact, our Proposition 1 formally nests that limiting possibility, which would amount to $R_{t+h|t,t-J}=0$ and thus effectively no distortion even if $\theta > 0$. In the BGS formulation that limit is imposed through a discontinuity at $\sigma_{t+h|t}^2 = 0$: in the language developed in Bordalo et al. (2018), to compute $\mathbb{E}_t^{\theta}(x_{t+h})$ the realization x_{t+h} constitutes its infinitely representative state (see appendix in Bordalo et al. (2018) on Corollary 1), and the result is $\mathbb{E}_{t}^{\theta}(x_{t+h}) = \mu_{t+h|t}$. Instead, under Smooth DE the effective overreaction $\theta_{t,t-J}$ in equation (10) smoothly goes to zero as current uncertainty goes to zero. Thus, the transition from distorted beliefs in the presence of uncertainty to non-distorted beliefs absent uncertainty occurs smoothly in the framework proposed here, as opposed to discontinuously, as in the original BGS formulation.³

³Smooth DE is built on the key informational difference between conditional (or posterior) and unconditional (prior) distribution information. In this sense, our approach relates to recent work in Bordalo et al. (2020), which features a sampling by similarity framework that under conditional probability assessments

Second, and more importantly, away from the zero conditional uncertainty case, in the original BGS formulation the ratio $R_{t+h|t,t-J}$ is always 1 because, by the BGS Assumption 2, the reference RE distribution differs from the current RE distribution only in terms of its mean, implying that the ratio of today's uncertainty to past uncertainty is always equal to 1. Thus, the proposed Smooth DE density nests the original specification of BGS. To see this, note that if $R_{t+h|t,t-J} = 1$, the effective overreaction $\tilde{\theta}_{t,t-J} = \theta$, and formulas (5) and (6) collapse to their respective counterparts in equations (8) and (9).

2.6 Overreaction to new information and Smooth DE

At its heart, representativeness leads decision-makers to overreact to new information. Smooth DE formalizes the interpretation of new information as a change in information sets. To further understand Smooth DE, we rewrite the distorted conditional mean and variance in Proposition 1 as a function of the revised information, as follows.

Corollary 2 (A revision representation). The Smooth DE density of Proposition 1 can be represented as distorting the RE revisions in conditional mean and variance, as follows:

$$\underbrace{\mathbb{E}_{t}^{\theta}\left(x_{t+h}\right) - \mu_{t+h|t-J}}_{Smooth\ DE\ revision} = \underbrace{\left(\mu_{t+h|t} - \mu_{t+h|t-J}\right)}_{RE\ revision}\underbrace{\left(1+\theta\right)}_{BGS\ effect}\underbrace{\left[1+\theta\left(1-R_{t+h|t,t-J}\right)\right]^{-1}}_{Smooth\ DE\ effect}$$

$$\underbrace{\frac{\mathbb{V}_{t}^{\theta}\left(x_{t+h}\right)}{\sigma_{t+h|t-J}^{2}}}_{Smooth\ DE\ revision} = \underbrace{\frac{\sigma_{t+h|t}^{2}}{\sigma_{t+h|t-J}^{2}}}_{RE\ revision} \underbrace{\left[1 + \theta\left(1 - R_{t+h|t,t-J}\right)\right]^{-1}}_{Smooth\ DE\ effect}$$

This representation indicates how the revision in conditional moments under Smooth DE can be decomposed as having three parts: (1) the RE revision, (2) an overreaction effect from representativeness as assumed in the standard BGS implementation of DE, and (3) a separate and novel effect stemming from Smooth DE.

In Figure 3 we use a series of illustrative examples to show the different effects at work in Corollary 2.⁴ In the first row, we report the reference, current, DE, and Smooth DE distributions. In the second row, we report the weights that capture the belief distortion

yields a result reminiscent of DE. In a similar spirit to Smooth DE, there it is also important to keep track of the entire prior distribution, which plays a major role in memory interference.

⁴We use the following parameter values for the mean and variances of the current and reference distributions: $\mu_{t+h|t-J} = [0, 0, 0, 0, 0], \ \mu_{t+h|t} = [1, 0, 0, 1, 1], \ \sigma_{t+h|t-J}^2 = [1, 1, 1, 1, 1], \ \text{and} \ \sigma_{t+h|t-J}^2 = [1, .5, 1.3, .5, 1.3].$

(2) $\Delta \sigma^2 < 0$ (4) $\Delta \mu > 0 \& \Delta \sigma^2 < 0$ 0.35 0.35 0.35 Densities c 25.0 0.3 0.8 0.25 0.25 0.6 0.2 0.6 0.15 0.15 0.1 0.1 0.1 0.2 0.2 0.05 30 0.5 Smooth DE --- DE - Reference ---- Current

Figure 3: Smooth Diagnostic Expectations and standard Diagnostic Expectations densities

Notes: The figure is obtained using the following parameter values for the mean and variances of the current and reference distributions: $\mu_{t+h|t-J} = [0,0,0,0,0]$, $\mu_{t+h|t} = [1,0,0,1,1]$, $\sigma^2_{t+h|t-J} = [1,1,1,1,1]$, and $\sigma^2_{t+h|t-J} = [1,.5,1.3,.5,1.3]$.

under DE and under Smooth DE. These are computed as:

Weight
$$(\widehat{x}_{t+h}) = \left(\frac{N(\widehat{x}_{t+h}; \mu_{t+h|t}, \sigma_{t+h|t}^2)}{N(\widehat{x}_{t+h}; \mu_{t+h|t-J}, \sigma_{t+h|t}^2)}\right)^{\theta} \frac{1}{Z},$$

for the standard DE and

Weight
$$(\widehat{x}_{t+h}) = \left(\frac{N(\widehat{x}_{t+h}; \mu_{t+h|t}, \sigma_{t+h|t}^2)}{N(\widehat{x}_{t+h}; \mu_{t+h|t-J}, \sigma_{t+h|t-J}^2)}\right)^{\theta} \frac{1}{Z},$$

for the Smooth DE.

Revision only in conditional mean. We first consider a case in which the reference and current distributions only differ in terms of the mean: $\mu_{t+h|t} > \mu_{t+h|t-J}$ and $R_{t+h|t,t-J} = 1$. This implies that the new information did not lead to any change in uncertainty. In this case, Corollary 2 indicates that the additional Smooth DE effect is absent. Therefore, Smooth DE and DE lead to the same distorted normal distribution, in which only the conditional mean is distorted. Both the SDE and DE means are shifted to the right with respect to the

current RE distribution by $\theta(\mu_{t+h|t} - \mu_{t+h|t-J})$. The lower panel in the first column shows that the weights increase as we move from left to right: The weights shift probability mass to the right of the current density, lowering the probability assigned to events that became less likely, and inflating the probability of events that became more likely. The weights keep increasing as elements in the right tail of the current RE density became much more likely to occur in relative terms. However, the RE probability of these events goes to zero faster than the weights increase, preserving the normality of the SDE and DE distributions.

Revisions only in conditional uncertainty. In the second and third columns, we consider two cases in which the reference and current distributions only differ in terms of variance, while keeping $\mu_{t+h|t} = \mu_{t+h|t-J}$. Corollary 2 shows that the absence of a revision in the RE conditional mean implies no revision in the distorted conditional mean, under both Smooth and Standard DE. However, Corollary 2 also indicates that Smooth DE implies a novel distortion in the revision of conditional uncertainty, that is absent under DE.

Specifically, in the second column the current RE distribution features a lower variance, i.e $\sigma_{t+h|t}^2 < \sigma_{t+h|t-J}^2$ and thus $R_{t+h|t,t-J} < 1$. This case is typical for standard stochastic processes when new information and a shorter time-horizon (i.e., h < h + J) lead to a reduction of uncertainty and more precise forecasts. Under the standard BGS implementation of DE, the change in variance does not lead to any change in the DE distribution. The weights are uniformly equal to 1, as illustrated by the dashed line in the second row of column 2. Under standard DE, the fact that events close to the mean, and the mean itself, became more likely does not have any effect. Instead, under Smooth DE, the agent revises her beliefs in light of the new information. She inflates the probability of the mean and the other events that became more representative, while further downplaying the probability of events that became less likely. The result is an even narrower distribution with respect to the current RE distribution. As indicated in Corollary 2, under Smooth DE, the new information leads to overreaction in terms of the decline in uncertainty and, as a result, to a novel implication: overconfidence.

The third case considers a situation in which the current distribution has a larger variance than the reference distribution, i.e. $\sigma_{t+h|t}^2 > \sigma_{t+h|t-J}^2$, and thus $R_{t+h|t,t-J} > 1$. This situation could arise, for example, in response to a positive uncertainty shock. Now tail events become more representative under the revised density and receive a magnified weight under Smooth DE. The probability mass is moved from the center to the tails, but preserving normality. This example also allows us to illustrate the role of the upper bound on $R_{t+h|t,t-J}$: As this ratio increases, more and more probability mass is moved to the tails, flattening the normal distribution. As $R_{t+h|t,t-J} \to (1+\theta)/\theta$, the variance of the Smooth DE density goes to infinity, as an increasing probability mass is moved to the tails. Under DE, the weights are

once again uniformly equal to 1, and the DE density coincides with the RE density.

Revisions in conditional uncertainty affect revisions in conditional mean. The fourth and fifth columns combine a revision in mean with a revision in variance. The key observation here is illustrated by the decomposition of the distorted conditional mean in Corollary 2: under Smooth DE, a change in uncertainty affects the degree to which the distorted revision responds to the RE revision. Since changes in information sets typically involve changes in both RE conditional moments, this is a particularly novel and important aspect of Smooth DE.

In particular, the fourth case combines the first two, with an increase in the conditional mean and a reduction of conditional uncertainty. As in the first case, under DE we observe a shift of the probability mass to the right. Accordingly, the DE density moves to the right, but with no change in shape with respect to the RE density. Under Smooth DE, instead, the agent recognizes that, despite the increase in the mean, the new information made tail events to the right less representative. Thus, for a given θ , the Smooth DE density still shifts to the right, but by a smaller amount, and becomes visibly more narrow, as the weights take into account the change in uncertainty.⁵

Finally, new information can also bring a shift in the mean, but now with *more* uncertainty. The last column considers this case, where the shift in the mean is positive like in the fourth column. The agent's overreaction in terms of revisions to the conditional mean is now *stronger* than under standard DE because tail events have become more likely under the current distribution. Thus, the weights determine an even more significant shift of probability mass to the right (the scale for the SDE weights is on the left). In terms of distorted conditional uncertainty, in this case, we observe underconfidence. This is again in itself a form of *overreaction*, as the agent magnifies the increase in uncertainty as this appears large compared to the reference uncertainty.

News and uncertainty. In Figure 4, we study how news and uncertainty effects determine the overreaction of the Smooth DE density relative to the posterior distribution. To facilitate comparison with Figure 3, we mark the coordinates corresponding to the prior mean and variance with white pluses, and the coordinates corresponding to the posterior means and variances of each scenario in Figure 3 with red circles. Panel (a) and (b) visually illustrate how the Smooth DE mean and variance change as the posterior mean and variance change and confirm our results in Corollary 1: panel(a) shows larger overreactions for higher posterior variances and panel (b) highlights overconfidence for posterior variances

⁵If the current conditional uncertainty would become continuously smaller and converge to zero, the shift in the distorted conditional mean also smoothly becomes smaller. In contrast, under standard DE, the shift would change only in the extreme case of $\sigma_{t+h|t=0}^2$, when it would become nil.

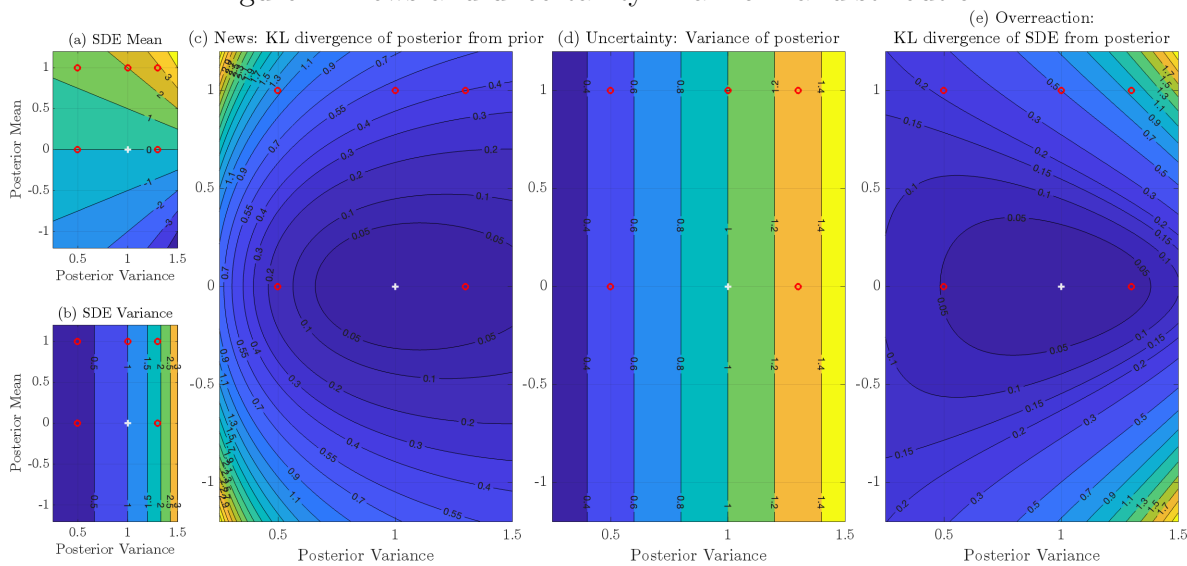


Figure 4: News and uncertainty in a Normal distribution

Notes: The figure displays how, as we vary the posterior mean and variance, the following objects change: (a) the Smooth DE mean, (b) the Smooth DE variance, (c) the news component, measured using the KL divergence of the posterior distribution from the prior distribution, (d) the uncertainty component, measured using the posterior variance, and (e) the overall overreaction, measured using the KL divergence of the Smooth DE distribution from the posterior distribution. We mark the coordinates corresponding to the prior mean and variance with white pluses, and the coordinates corresponding to the posterior means and variances of each scenario in Figure 3 with red circles.

lower than the prior variance and underconfidence for posterior variances higher than the prior variance. Panel (c) shows the news effect, measured in terms of the KL divergence of the posterior distribution from the prior distribution. Interestingly, the KL divergence is large when the posterior variance is low and there is a large shift in the mean. The news effect is large in that case because we are moving probability masses of tail events under the prior distribution. In contrast, the uncertainty effect is large when the posterior variance is high (panel (d)). Panel (e) shows that the uncertainty effect of higher posterior variance dominates the news effect, so the overreaction of the Smooth DE density (measured in terms of the KL divergence of the Smooth DE density to posterior density) is largest when there is a large shift in the mean and an increase in variance.

2.7 Some examples of stochastic processes

We illustrate the tractability of Smooth DE for some standard stochastic processes. For a simpler exposition we focus on the one-step-ahead horizon (h = 1) and recent past (J = 1).

2.7.1 AR(1) process

Like in the original BGS DE formulation, the Smooth DE density derived above can be easily applied in the standard case of an AR(1) process. Consider

$$x_{t+1} = \rho x_t + \varepsilon_{t+1}, \quad \varepsilon_{t+1} \sim \mathcal{N}(0, \sigma^2)$$
 (15)

where $\rho \leq 1$ and $\sigma^2 > 0$. The true conditional density is simply

$$f(\widehat{x}_{t+1}|\mathcal{I}_t) = \mathcal{N}(\widehat{x}_{t+1}; \rho x_t, \sigma^2)$$
.

The reference density is the counterpart of equation (3)

$$f\left(\widehat{x}_{t+h}|\mathcal{I}_{t-J}^{\text{ref}}\right) = \mathcal{N}\left(\widehat{x}_{t+h}; \rho^2 x_{t-1}, \left(1+\rho^2\right)\sigma^2\right)$$

As a result, $R_{t+1|t,t-1}$ defined in Proposition 2 takes the form

$$R_{t+1|t,t-1} = \frac{\sigma^2}{(1+\rho^2)\,\sigma^2} \tag{16}$$

The Smooth DE density $h^{\theta}\left(\widehat{x}_{t+1}\right)$ in Proposition 1 is then Normal, with a conditional mean

$$\mathbb{E}_{t}^{\theta}(x_{t+1}) = \rho x_{t} + \frac{\theta}{1 + \rho^{2}(1+\theta)} \left(\rho x_{t} - \rho^{2} x_{t-1}\right)$$
(17)

and conditional distorted variance

$$\mathbb{V}_t^{\theta}\left(x_{t+1}\right) = \frac{\sigma^2}{1 + \frac{\rho^2}{1 + \sigma^2}\theta} \tag{18}$$

This AR(1) example illustrates well some of the general principles behind Smooth DE. First, as long as $\theta > 0$, Smooth DE exhibits a positive effective overreaction in equation (17) of the conditional mean to news. Second, given σ^2 , a higher persistence parameter ρ implies that the new information determines a larger reduction in current uncertainty about the variable of interest x_{t+1} compared to the reference density. This lower variance ratio $R_{t+1|t,t-1}$ leaves less room for memory to distort probability judgements which makes the effective overreaction in equation (17) decrease in the persistence parameter ρ . Third, since new information at time t lowers the conditional uncertainty from $(1 + \rho^2) \sigma^2$ to σ^2 , the ratio $R_{t+1|t,t-1} < 1$ in equation (16). Thus, the distorted density is characterized by overconfidence, so that $\mathbb{V}^{\theta}_t(x_{t+1}) < \sigma^2$, as seen in equation (18), and the level of overconfidence is increasing

in the persistence of the process as captured by ρ .

2.7.2 Signal extraction under Smooth DE

An important class of models emphasizing changes in subjective uncertainty belongs to the large literature on Bayesian learning. In what follows, we incorporate Smooth DE within this class of models, and use the resulting framework to connect to survey data.

Consider a standard state-space representation. The observation equation is:

$$s_t = x_t + \varepsilon_t, \qquad \varepsilon_t \sim N(0, \sigma_{\varepsilon}^2)$$

and the state transition equation for the unobserved x_t is

$$x_t = \rho x_{t-1} + u_t, \qquad u_t \sim N(0, \sigma_u^2)$$

The Kalman Filter derived under RE is standard. The one-step-ahead prediction from the period t-1 estimate $\tilde{x}_{t-1|t-1}$ and its associated error variance $\Sigma_{t-1|t-1}$ are given by

$$\tilde{x}_{t|t-1} = \rho \tilde{x}_{t-1|t-1}; \Sigma_{t|t-1} = \rho^2 \Sigma_{t-1|t-1} + \sigma_u^2.$$

Then, the estimates are updated according to

$$\tilde{x}_{t|t} = \tilde{x}_{t|t-1} + K_t(s_t - \tilde{x}_{t|t-1}), \qquad K_t = \frac{\sum_{t|t-1}}{\sum_{t|t-1} + \sigma_{\varepsilon}^2},$$

where K_t is the Kalman gain and the updating rule for the variance is

$$\Sigma_{t|t} = \left[\frac{\sigma_{\varepsilon}^2}{\Sigma_{t|t-1} + \sigma_{\varepsilon}^2}\right] \Sigma_{t|t-1}.$$
 (19)

Smooth Diagnostic Kalman filter. We extend the diagnostic Kalman filter derived within the standard BGS formulation in earlier work like Bordalo et al. (2019) and Bordalo et al. (2020) to the case of Smooth DE.

Let $f_t(x_t)$ be the probability density of the rational, or Bayesian, period t estimate of the underlying state x_t . Define the representativeness of state x at period t as:

$$rep_t(x_t) = f_t(x_t)/f_{t-1}(x_t)$$

Intuitively, a state x_t is more representative if it becomes more likely relative to the t-1 forecast. As in our discussion of equation (2), the key feature with respect to the original

BGS formulation is to condition on the whole past information set, and as a result, to take into account the associated *uncertainty*.

The posterior is then distorted using the following Smooth DE density:

$$f_t^{\theta}(x_t) = f_t(x_t) \left[rep_t(x_t) \right]^{\theta} (1/Z),$$
 (20)

where Z is a normalizing constant so that $f_t^{\theta}(x_t)$ integrates to one.

Let the ratio of current to prior estimation uncertainty under RE be denoted as

$$R_{t|t,t-1} \equiv \Sigma_{t|t}/\Sigma_{t|t-1}$$
.

We derive the following result.

Proposition 3 (Smooth DE Kalman Filter.) The density $f_t^{\theta}(x_t)$ in equation (20) has a Normal distribution with mean

$$\mathbb{E}_{t}^{\theta}(x_{t}) = \tilde{x}_{t|t} + \frac{R_{t|t,t-1}\theta}{1 + (1 - R_{t|t,t-1})\theta} \left(\tilde{x}_{t|t} - \tilde{x}_{t|t-1}\right), \tag{21}$$

and variance

$$\mathbb{V}_t^{\theta}\left(x_t\right) = \frac{\Sigma_{t|t}}{1 + \left(1 - R_{t|t,t-1}\right)\theta} \tag{22}$$

Proof. See Appendix.

Like in our earlier general discussion, we observe overreaction of the conditional mean when $\theta > 0$ and the new information does not fully resolve uncertainty, i.e. when $\sigma_{\varepsilon}^2 > 0$. Furthermore, similarly to the earlier AR(1) example, this environment is also characterized by a conditional reduction in uncertainty, and therefore by overconfidence. Indeed, as long as σ_{ε}^2 is finite, by equation (19) estimation uncertainty decreases over time, as the new signal is at least partly informative. It follows that the ratio $R_{t|t,t-1} < 1, \forall t$ and that given equation (22), subjective uncertainty is lower than Bayesian estimation uncertainty, i.e. $\mathbb{V}_t^{\theta}(x_t) < \Sigma_{t|t}$.

3 A parsimonious micro-foundation for survey evidence

Like in existing work on DE, we take the underlying $\theta \geq 0$ and $J \geq 1$ as primitive parameters characterizing the decision's maker limited memory and the effect that the representativeness heuristic has on agent's judgments. As discussed in Section 2, given θ and J, the Smooth DE density does not introduce any further degress of freedom. Nevertheless, by allowing the density for the representative group to reflect the time t-J conditional uncertainty, we

find that Smooth DE can offer a *joint and parsimonious micro-foundation* for a range of observable implications consistent with survey data. These implications refer to the broad properties of Smooth DE emphasized and collected by Corollary 1.

At its core, Smooth DE captures the intuition that new information that significantly reduces current uncertainty over the variable of interest leaves less room for memory and representativeness to distort judgements. As we discuss below, this implication of a stronger (weaker) effective overreaction of the conditional mean to new information that reduces less (more) current uncertainty helps to account for two sets of stylized survey facts.

3.1 Stronger overreaction for longer forecast horizons

The first set of over-identifying restrictions on our theory of overreaction relates to the model's implications for short- versus long-horizon forecasts. A strand of literature using survey data argues that overreaction appears to be increasing with the horizon of the forecast. For example, Bordalo et al. (2019) and Bordalo et al. (2023) point to such stronger overreaction for equity analysts' forecasts of long-term earnings growth and emphasize the potential for this type of overreaction to account for stock market volatility. Using professional forecasters' forecasts of interest rates, other contributions, including for example Bordalo et al. (2020), d'Arienzo (2020), find evidence of significant overreaction for expectations of long-term interest rates, but not for expectations of short-term interest rates. Augenblick et al. (2021) use field data from betting and financial markets to argue that compared to the Bayesian forecast there is relatively stronger overreaction to signals with a longer (shorter) time-to-resolution, conceptually similar to longer (shorter) forecast horizons.

Smooth DE is consistent with such evidence as it by predicts that overreaction increases with the horizon of the forecast. The basic intuition appears in Section 2. Smooth DE formalizes an inverse relation between the informativeness of the new piece of information obtained by the decision-maker and the overreaction of her conditional forecasts (see for example equation (12) in Corollary 1). In the context of forecasting at different horizons, the same piece of information is less informative about horizons further in the future, leading to a smaller reduction in uncertainty and a stronger overreaction. Thus, Smooth DE naturally predicts that overreaction is relatively stronger for long-horizon forecasts.

The simplest environment to showcase this basic insight is the AR(1) process introduced with equation (15) in Section 2. For an horizon $h \ge 1$ and a J- lagged reference distribution $(J \ge 1)$, the conditional mean for the Smooth DE density $f^{\theta}(\widehat{x}_{t+h})$ is

$$\mathbb{E}_{t}^{\theta}\left(x_{t+h}\right) = \rho^{h} x_{t} + \widetilde{\theta}_{t,t-J} \left(\rho^{h} x_{t} - \rho^{h+J} x_{t-J}\right) \tag{23}$$

where the effective severity $\widetilde{\theta}_{t,t-J}$ of DE distortion is given in equation (10).

Given the AR(1) process in equation (15), the ratio $R_{t+h|t,t-J}$ of conditional variances, defined in Proposition 1, takes the particular form

$$R_{t+h|t,t-J} = \frac{\mathbb{V}_t [x_{t+h}]}{\mathbb{V}_{t-J} [x_{t+h}]} = \begin{bmatrix} \frac{1-\rho^{2h}}{1-\rho^{2(h+J)}} & \text{when } \rho^2 < 1\\ \frac{h}{h+J} & \text{when } \rho^2 = 1 \end{bmatrix}$$

Proposition 4 The ratio $R_{t+h|t,t-J}$ increases in the forecast horizon h. Thus, the effective overreaction $\widetilde{\theta}_{t,t-J}$ of $\mathbb{E}^{\theta}_{t}(x_{t+h})$ in equation (23) is stronger for longer forecast horizons.

For a given lag J in the reference distribution, as the forecast horizon h increases, the effective horizon of the current RE forecast (h), and the effective horizon of the reference RE forecast (h + J) become increasingly similar. As a result, the levels of uncertainty associated with the two forecasts also become increasingly similar because the information set is implicitly more similar. Intuitively, the uncertainty around the two forecasts reflects a larger and larger number of the same shocks. In relative terms, the current information set is less and less informative for the variable that the agent is trying to predict. Given that under Smooth DE overreaction is increasing in the level of relative uncertainty, as h increases, so does the amount of overreaction to a given revision of the RE forecasts.

3.2 Stronger overreaction for weaker signals

The same logic of differential overreaction as a function of the informativeness of signals connects to a second set of facts, documented recently in Augenblick et al. (2021). That work, using experimental evidence, finds that, compared to Bayesian forecasts, decision-makers (1) overreact to weaker signals and (2) underreact to stronger signals. To formalize the argument, we build on the Smooth DE filtering setup of Section 2.7.2 and connect to the experimental setup of Augenblick et al. (2021) as follows.

First, we let the true process be described as noisy signals over some $x_t \sim N(0, \sigma_x^2)$, with $\sigma_x^2 > 0$. In particular, weak and strong signals are respectively defined as

$$s_{W,t}^* = x_t + \varepsilon_{W,t}^*, \qquad \varepsilon_{W,t}^* \sim N(0, \sigma_W^2)$$

$$s_{S,t}^* = x_t + \varepsilon_{S,t}^*, \qquad \varepsilon_{S,t}^* \sim N(0, \sigma_S^2)$$

where we model objectively weak signals as being more noisy than strong signals by assuming

$$\sigma_W^2 > \sigma_S^2 > 0.$$

The conditional Bayesian forecasts formed by an econometrician are then

$$\mathbb{E}^* (x_t | s_{W,t}^*) = K_W^* s_{W,t}^*, \qquad \mathbb{E}^* (x_t | s_{S,t}^*) = K_S^* s_{S,t}^*$$
(24)

where the corresponding signal-to-noise ratios satisfy

$$0 < K_W^* = \frac{\sigma_x^2}{\sigma_x^2 + \sigma_W^2} < K_S^* = \frac{\sigma_x^2}{\sigma_x^2 + \sigma_S^2} < 1$$

Second, representativeness is a model of overreaction of the conditional mean to news, irrespective of how informative the latter is (see for example Corollary 1). To connect to the evidence in Augenblick et al. (2021), which finds underreaction (to stronger signals), we thus add subjective noise perceived by the decision-maker. As a result, the signals as perceived by the agent, as opposed to drawn under the true process, are:

$$s_{W,t} = s_{W,t}^* + \varepsilon_t^c, \quad s_{S,t} = s_{S,t}^* + \varepsilon_t^c, \quad \varepsilon_t^c \sim N(0, \sigma_{\varepsilon,c}^2)$$

The randomness ε_t^c captures cognitive noise, arising from limited attention or cognition (see eg. Woodford (2001)). We keep this cognitive noise symmetric: both objectively weak and strong signals are subject to the same amount of cognitive noise, governed by $\sigma_{\varepsilon,c}^2 > 0$. The resulting signal-to-noise ratios used by the agent in forming conditional forecasts satisfy

$$K_W = \frac{\sigma_x^2}{\sigma_x^2 + \sigma_W^2 + \sigma_{\varepsilon,c}^2} < K_W^*, \qquad K_S = \frac{\sigma_x^2}{\sigma_x^2 + \sigma_S^2 + \sigma_{\varepsilon,c}^2} < K_S^*$$
 (25)

Since the agent understands that she faces cognition noise, her subjective conditional forecasts of x_t underreacts to the true $s_{W,t}^*$ and $s_{S,t}^*$ compared to the econometrician. Formally, this is evident by the inequalities in equations (25). Thus, without Smooth DE, she would underreact to both weak and strong signals, in contrast to the evidence. Thus, the key modeling ingredient is to *introduce Smooth DE* in this environment. Proposition 3 can be used to derive conditional forecasts under Smooth DE, here made further tractable by the maintained iid assumptions, as follows:

$$\mathbb{E}^{\theta} \left(x_t | s_{W,t} \right) = \left[1 + \frac{\theta (1 - K_W)}{1 + \theta K_W} \right] K_W s_{W,t}$$

$$\mathbb{E}^{\theta} \left(x_t | s_{S,t} \right) = \left[1 + \frac{\theta (1 - K_S)}{1 + \theta K_S} \right] K_S s_{S,t}$$

Comparing the above responses of conditional forecasts under Smooth DE to those formed by the econometrician in equation (24), we can establish the following result: **Proposition 5** (Weak vs. strong signal reaction). Given some amount $\sigma_{\varepsilon,c}^2 > 0$ of cognitive noise, if the noise variances of weak and strong signals satisfy the following inequalities

$$\sigma_W^2 > \frac{\sigma_{\varepsilon,c}^2}{\theta} > \sigma_S^2 \tag{26}$$

the agent's conditional forecasts overreact to weak signals compared to the Bayesian forecast:

$$\frac{\partial \mathbb{E}^{\theta} \left(x_{t} | s_{W,t} \right)}{\partial s_{Wt}^{*}} > \frac{\partial \mathbb{E}^{*} \left(x_{t} | s_{W,t}^{*} \right)}{\partial s_{Wt}^{*}}$$

$$(27)$$

while at the same time they underreact to strong signals:

$$\frac{\partial \mathbb{E}^{\theta} \left(x_{t} \middle| s_{S,t} \right)}{\partial s_{S,t}^{*}} < \frac{\partial \mathbb{E}^{*} \left(x_{t} \middle| s_{S,t}^{*} \right)}{\partial s_{S,t}^{*}} \tag{28}$$

Proof. See Appendix.

Intuitively, compared to the econometrician's forecast, representativeness produces overreaction, while the presence of cognitive noise leads to underreaction. Consider first weak
signals. When the representativeness effect is stronger than the cognitive noise effect, summarized by the first parameter inequality in equation (26), we obtain a measured overreaction,
as evident in equation (27). However, if that level of representativeness effect were to apply equally to strong signals, as implied by standard DE, then we would also measure the
same overreaction to strong signals, in contrast to the evidence. Instead, with Smooth DE,
stronger signals reduce agents' conditional uncertainty more than weaker signals, and thus
dampen the representativeness effect on forecasts. Thus, the cognitive noise effect can be
relatively more powerful for stronger signals (when the second inequality in equation (26)
is satisfied), leading to measured underreaction in equation (28). These joint properties are
consistent with the experimental evidence in Augenblick et al. (2021).

3.3 overreaction and overconfidence

A recent literature studying the properties of survey responses, including Barrero (2022), Born et al. (2022), and the recent reviews in Altig et al. (2020) and Born et al. (2022), documents that while firms' forecasts are unconditionally unbiased, i.e forecast errors are on average not significantly different from zero, firms make conditionally predictable forecast errors. In particular, firms (a) overreact to news and (b) are overconfident in their subjective forecasts.

These stylized facts provide a challenge for models featuring standard rational belief

updating. As a result, the overreaction and overconfidence empirical properties have been typically addressed in existing models through two distinct behavioral primitive assumptions that do not distort unconditional forecasts. overreaction of conditional forecasts has been explained as an outcome of DE, modelled according to the original BGS formulation. Under DE, agents overreact only in presence of new information and in a symmetric way, preserving unbiased unconditional forecasts, but failing to account for overconfidence. Thus, the finding of overconfidence has been typically addressed with an additional overconfidence bias (as reviewed above). An example of this approach is Barrero (2022), who uses both distinct features to account for the three survey facts.

Smooth DE can instead account for all three stylized facts. Consider for example the Gaussian environment of Section 2 where a firm's fundamental (eg. productivity) follows a simple AR(1) process. Or, the arguably more empirically plausible extension, where those fundamentals are not directly observed, but firms can learn about their realizations from noisy signals, like in the simple state-space model described in Section 2.7.2. In either case, Corollary 1 and Proposition 3, respectively, describe how forecasts made under Smooth DE are characterized by precisely these two key properties: overreaction to news and overconfidence. Moreover, as in the RE case ($\theta = 0$), forecasts under DE are nevertheless unconditionally unbiased, being on average driven by the underlying rational forecasts.

The discussion and formalism in Section 2 indicate that, in contrast to the generality of the overreaction of the conditional mean, overconfidence is not a universal property of Smooth DE. However, we view it as a 'typical' property, because the necessary condition for overconfidence is simply that new information reduces uncertainty. This condition is ubiquitous as it holds in stationary, homoskedastic environments, where events closer into the future are naturally easier to predict than events far into the future. At the same time, the condition might not hold if new information entails a sufficiently large and unexpected increase in uncertainty, as indicated by some of our examples in Figure 3.

Finally, we further note the broader context of a large literature on overconfidence (eg. De Bondt and Thaler (1995) and Daniel et al. (1998, 2001)). This work has been motivated by extensive psychological evidence for overconfidence and argues that models based on this behavioral property are promising in accounting for asset market puzzles. Our key insight here is that Smooth DE emerges as a potential parsimonious micro-foundation, based on the representativeness heuristic, for overreaction and overconfidence, two behavioral features argued as important in understanding a variety of economic outcomes.⁶

 $^{^6}$ See further Barberis (2018) for a review of these two-widely documented, but typically studied separately, departures from standard Bayesian updating.

4 Business cycle implications

We illustrate the business cycle implications of Smooth DE in a parsimonious RBC model with time-varying uncertainty. We argue that Smooth DE emerges as a novel behavioral propagation and amplification mechanism for time-varying uncertainty. We first show that the model replicates, without relying on additional frictions, several salient features of data thanks to the state-dependent overreaction: (1) asymmetry (recessions are deeper than expansions), (2) countercyclical micro volatility (cross-sectional variances of microeconomic variables rise in recessions), and (3) countercyclical macro volatility (time-series variances of macroeconomic variables rise in recessions). We also show that, the perceived increase of uncertainty in recessions is more than three times larger than the actual uncertainty increase. We then discuss a novel policy implication: a redistributive policy that reduces idiosyncratic uncertainty could be beneficial for macroeconomic stabilization because it dampens the state-dependent overreaction.

4.1 The model

To isolate and highlight the role of Smooth DE as a propagation mechanism, we keep the model simple and abstract from conventional frictions in the uncertainty shock literature, such as adjustment costs (Bloom (2009) and Bloom et al. (2018)) and sticky prices (Basu and Bundick (2017) and Fernández-Villaverde et al. (2015)). The economy consists of a continuum of islands $i \in [0, 1]$. In each island i, an agent has the following per-period utility function

$$U(c_{i,t}, h_{i,t}) = \frac{c_{i,t}^{1-\gamma}}{1-\gamma} - \beta \frac{h_{i,t}^{1+\eta}}{1+\eta}.$$

where $c_{i,t}$ is consumption, $h_{i,t}$ is the amount of hours worked, γ is the coefficient of relative risk aversion, and η is the inverse of the Frisch labor elasticity. We simplify the algebra below by multiplying the disutility of labor by the discount factor β .

Output in each island is produced according to

$$y_{i,t} = z_{i,t} h_{i,t-1}. (29)$$

The t-1 subscript on hours reflects the assumption that the labor input is chosen before

⁷As described in the Introduction, these properties have strong empirical support in the literature. The concept of asymmetries have a long tradition in macroeconomics, including Neftci (1984), Hamilton (1989), Sichel (1993), and more recently McKay and Reis (2008) and Morley and Piger (2012). The extensive literature of the macroeconomics of time-varying uncertainty, including Bloom (2009), Fernández-Villaverde et al. (2011), Ilut et al. (2018), Jurado et al. (2015), Basu and Bundick (2017), and Bloom et al. (2018) confirm that volatility or uncertainty is countercyclical at both micro and macro levels.

the random realization of productivity $z_{i,t}$ is known. The island resource constraint is

$$c_{i,t} = y_{i,t}. (30)$$

We obtain aggregate variables by simply adding up variables of all islands:

$$H_t = \int_0^1 h_{i,t} di, \quad Y_t = \int_0^1 y_{i,t} di, \quad C_t = \int_0^1 c_{i,t} di$$

The island productivity $z_{i,t+1}$ is the sum of aggregate and idiosyncratic components:

$$\ln z_{i,t+1} = A_{t+1} + a_{i,t+1},$$

The economy-wide TFP shock A_{t+1} is common across all islands and follows the process

$$A_{t+1} = \rho_A A_t + u_{A,t+1}, \quad u_{A,t+1} \sim i.i.d.N(0, \sigma_A^2).$$

The idiosyncratic TFP $a_{i,t+1}$ is instead specific to island i, and it is composed of a predictable component $s_{i,t} \sim i.i.d.N(0, \sigma_s^2)$, known one-period-in-advance, and an unpredictable component $u_{a,i,t+1} \sim i.i.d.N(0, \sigma_{a,t}^2)$ realized at t+1:

$$a_{i,t+1} = s_{i,t} + u_{a,i,t+1}.$$

Following Bloom et al. (2018), we assume the volatility $\sigma_{a,t}$ is time-varying and negatively correlated with the economy-wide TFP. In particular, as we describe in Section 4.4, $\sigma_{a,t}$ increases when there is a negative innovation to the economy-wide TFP, and vice versa. We use $\sigma_{a,t}$ to denote the volatility of the period t+1 innovation to reflect the assumption that the volatility of the next period's innovation is known one-period-in-advance. We also assume that the volatility of the predictable component, $s_{i,t}$, is constant. This implies that the cross-sectional dispersion of labor is driven only by the news effect of the uncertainty shock. If we were to relax the assumption of constant volatility of $s_{i,t}$, the cross-sectional dispersion would also depend on its realized volatility, but none of the main qualitative properties of the model would change.

The conditional posterior mean and variance of $a_{i,t+1}$ after observing the predictable component $s_{i,t}$ are given by

$$\mathbb{E}_{i,t}[a_{i,t+1}] = s_{i,t}, \quad \mathbb{V}_{i,t}[a_{i,t+1}] = \sigma_{a,t}^2.$$

We can define the residual uncertainty (posterior variance relative to ex-ante uncertainty)

as in David et al. (2016) as $\sigma_{a,t}^2/(\sigma_s^2 + \sigma_{a,t}^2)$, which is increasing in $\sigma_{a,t}^2$. Intuitively, in times of low aggregate TFP and higher uncertainty $\sigma_{a,t}^2$, the predictable component $s_{i,t}$ serves as a weaker signal in forecasting $a_{i,t+1}$ relative to times of lower uncertainty.

4.2 RE solution

We first characterize the equilibrium under Rational Expectations (RE). The island i agent's Bellman equation is given by

$$V(h_{i,t-1}, z_{i,t}) = \max_{h_{i,t}} \{ U(c_{i,t}, h_{i,t}) + \beta \mathbb{E}_{i,t} \left[V(h_{i,t}, z_{i,t+1}) \right] \},$$

subject to $y_{i,t} = z_{i,t}h_{i,t-1}$ and $c_{i,t} = y_{i,t}$.

Combining the first order condition for labor with the envelope condition, we obtain

$$(h_{i,t})^{\eta} = \mathbb{E}_{i,t} \left[(c_{i,t+1})^{-\gamma} z_{i,t+1} \right].$$
 (31)

The optimality condition equates the current marginal disutility of working with its expected benefit. The latter is given by the marginal product of labor weighted by the marginal utility of consumption. We log-linearize the condition and use the method of undetermined coefficients to obtain the RE solution.

Proposition 6 Using hats to denote log-deviations from the steady state, the equilibrium under RE is given as follows:

1. Individual hours worked are given by

$$\widehat{h}_{i,t} = \varepsilon \left[\rho_A A_t + s_{i,t} \right],$$

where

$$\varepsilon = \frac{1 - \gamma}{\eta + \gamma}.$$

Equilibrium output and consumption follow immediately as

$$\widehat{y}_{i,t} = A_t + a_{i,t} + \widehat{h}_{i,t-1} = \widehat{c}_{i,t}.$$

2. Equilibrium aggregate variables are given by

$$\widehat{H}_t = \varepsilon \rho_A A_t, \quad \widehat{Y}_t = A_t + \widehat{H}_{t-1} = \widehat{C}_t$$

Proof. See Appendix.

The response of individual and aggregate hours to news about expected economy-wide productivity $\rho_A A_t$ and island-specific productivity $s_{i,t}$ is affected by the intertemporal elasticity of consumption (IES), which here also equals the inverse of the coefficient of relative risk aversion. When the IES is large enough, so that $\gamma^{-1} > 1$ and thus $\varepsilon > 0$, an increase in expected productivity raises hours. In that case the intertemporal substitution effects dominates the wealth effect that would lower hours through the effect on marginal utility.

The next proposition characterizes the cross-sectional variance under RE.

Proposition 7 The cross-sectional variance of hours worked is given by

$$\int_0^1 \left(\widehat{h}_{i,t} - \widehat{H}_t \right)^2 di = \left[\frac{1 - \gamma}{\eta + \gamma} \right]^2 \sigma_s^2,$$

and is constant over the business cycle. The cross-sectional variances of output $y_{i,t}$ and consumption $c_{i,t}$ are increasing in the volatility $\sigma_{a,t-1}^2$ of the idiosyncratic TFP.

Proof. See Appendix.

Under RE, the cross-sectional variance of hours stays constant over the business cycle. This is because once the model is linearized, the news effect of changes in uncertainty is muted under RE. The cross-sectional variances of output and consumption are instead mechanically affected by $\sigma_{a,t-1}^2$ because of the change in realized volatility.

4.3 Smooth DE solution

We now solve the model under Smooth DE. We consider the case of distant memory, meaning that agents' memory recall is based on a more distant past, rather than just the immediate past. In terms of Assumption 1, this means that the reference group is based on the information set available J>1 periods ago. Bianchi et al. (2024) find that in standard models, distant memory can account for salient features of data, such as persistence and repeated boom-bust cycles. However, under distant memory, a time-inconsistency problem arises due to the failure of the law of iterated expectations. Bianchi et al. (2024) address this issue by adopting the $na\"{i}vet\'{e}$ approach (e.g. O'Donoghue and Rabin (1999)), which we also follow here. Under this approach, the agent fails to take into account that her preferences are time-inconsistent and thinks that in the future she will make choices under perfect memory recall, or RE. However, when the future arrives, the agent ends up changing behavior and be again subject to her imperfect memory recall.⁸

⁸In Bianchi et al. (2024) we further argue that the naïveté approach is psychologically coherent and consistent with the underlying foundation of diagnostic beliefs as a heuristic and a mental short-cut.

Let θ -superscripts and RE-superscripts denote equilibrium Smooth DE choices and choices under a RE policy function, respectively. The island i agent's Bellman equation is

$$\max_{h_{i,t}^{\theta}} \left\{ U(c_{i,t}^{\theta}, h_{i,t}^{\theta}) + \beta \mathbb{E}_{i,t}^{\theta} \left[\mathcal{V}(h_{i,t}^{\theta}, z_{i,t+1}) \right] \right\},$$

subject to $y_{i,t}^{\theta} = z_{i,t} h_{i,t-1}^{\theta}$ and $c_{i,t}^{\theta} = y_{i,t}^{\theta}$. The continuation value is given by

$$\mathcal{V}(h_{i,t-1}^{\theta}, z_{i,t}) = \max_{h_{i,t}^{RE}} \left\{ U(c_{i,t}^{RE}, h_{i,t}^{RE}) + \beta \mathbb{E}_{i,t} \left[\mathcal{V}(h_{i,t}^{RE}, z_{i,t+1}) \right] \right\},$$

subject to $y_{i,t}^{RE} = z_{i,t} h_{i,t-1}^{\theta}$ and $c_{i,t}^{RE} = y_{i,t}^{RE}$.

Similar to the RE problem, the agent optimally equates the marginal disutility of labor with its expected benefit, except that the benefit is evaluated under Smooth DE:

$$\left(h_{i,t}^{\theta}\right)^{\eta} = \mathbb{E}_{i,t}^{\theta} \left[\left(c_{i,t+1}^{RE}\right)^{-\gamma} z_{i,t+1} \right]. \tag{32}$$

Proposition 8 The equilibrium under Smooth DE is given as follows:

1. Individual hours worked are given by

$$\widehat{h}_{i,t}^{\theta} = \varepsilon \left[\rho_A A_t + s_{i,t} \right] + \frac{\widetilde{\theta}_{t,t-J} \eta}{\eta + \left(1 + \widetilde{\theta}_{t,t-J} \right) \gamma} \varepsilon \left[\rho_A \mathbb{N}_{t-J,t} \left[A_t \right] + s_{i,t} \right],$$
(33)

where ε is given in Proposition 6 and $\mathbb{N}_{t-J,t}[A_t] \equiv A_t - \mathbb{E}_{t-J}[A_t]$ represents the news in A_t , compared to past expectation. Equilibrium output and consumption follow as

$$\hat{y}_{i,t}^{\theta} = A_t + a_{i,t} + \hat{h}_{i,t-1}^{\theta} = \hat{c}_{i,t}^{\theta}. \tag{34}$$

2. The effective diagnosticity parameter $\widetilde{\theta}_{t,t-J}$ is given by

$$\widetilde{\theta}_{t,t-J} = \frac{R_{t+1|t,t-J}\theta}{1 + (1 - R_{t+1|t,t-J})\theta},$$
(35)

where

$$R_{t+1|t,t-J} = \frac{\mathbb{V}_{i,t} \left(-\gamma \widehat{c}_{i,t+1}^{RE} + A_{t+1} + a_{i,t+1} \right)}{\mathbb{V}_{i,t-J} \left(-\gamma \widehat{c}_{i,t+1}^{RE} + A_{t+1} + a_{i,t+1} \right)}.$$
 (36)

3. Equilibrium aggregate variables are given by

$$\widehat{H}_{t}^{\theta} = \varepsilon \rho_{A} A_{t} + \frac{\widetilde{\theta}_{t,t-J} \eta}{\eta + \left(1 + \widetilde{\theta}_{t,t-J}\right) \gamma} \varepsilon \rho_{A} \mathbb{N}_{t-J,t} \left[A_{t}\right]$$

$$\widehat{Y}_{t}^{\theta} = A_{t} + \widehat{H}_{t-1}^{\theta} = \widehat{C}_{t}^{\theta}$$

$$(37)$$

Proof. See Appendix.

First, consider the policy function for individual hours $h_{i,t}^{\theta}$. The first line of (33) is identical to the RE policy function. The second line captures the overreaction to news, i.e. surprises. Consider, for instance, a positive surprise to an economy-wide TFP A_t . Smooth diagnostic agents are over-influenced by this surprise and become over-optimistic about the future benefit of working, and hence work more (if $\varepsilon > 0$). The coefficient on this overreaction, $\frac{\tilde{\theta}_{t,t-J}\eta}{\eta+(1+\tilde{\theta}_{t,t-J})\gamma}$, is increasing in the effective diagnosticity $\tilde{\theta}_{t,t-J}$. From (34) individual output and consumption also overreact when individual hours overreact. Second, the effective diagnosticity $\tilde{\theta}_{t,t-J}$ is positively related to $R_{t+1|t-J}$, given by (36): the ratio between the current uncertainty about the (log-linearized) marginal benefit of labor and the uncertainty perceived at period t-J. Third, aggregate hours, output, and consumption also feature overreaction, controlled by $\tilde{\theta}_{t,t-J}$, to news about economy-wide shocks.

The expressions (35) and (36) in Proposition 8 suggest that an increase in uncertainty about future idiosyncratic productivity could raise $\tilde{\theta}_{t,t-J}$ and, in turn, the overreaction to news.¹⁰ The Proposition below indeed confirms this is the case.

Proposition 9 An increase in the volatility $\sigma_{a,t}^2$ of idosyncratic TFP raises the effective diagnosticity parameter $\tilde{\theta}_{t,t-J}$.

Proof. See Appendix.

There are two important implications of this proposition. First, the business cycle is asymmetric, even if the underlying shocks are symmetric. A positive TFP shock would lower uncertainty and, as result, overreaction. In contrast, a negative TFP shock would raise uncertainty and, as result, overreaction. Thus, a drop in economic activity in response

⁹Note that, for $s_{i,t}$, since it is i.i.d., the surprise is $s_{i,t}$ itself.

 $^{^{10}}$ In the current model, we must take a stance on how agents deal with time-varying volatility when forming expectations. There are two approaches to compute the conditional variance at t-J in (36) that preserve normality of the Smooth DE density. The first approach consists of making an "anticipated utility" assumption (Kreps (1998)). In this case, agents' uncertainty depends on the volatility at the time of the forecast, disregarding the possibility of volatility changes. The second approach consists of assuming that agents take into account the possibility of volatility changes, but that memory retrieves a Normal approximation of the resulting mixture of Normal's. We adopt the first approach, as it is arguably more consistent with the naïveté assumption and the general motivation of DE as a mental heuristics.

to a negative shock would be sharper, while an expansion in response to a symmetric positive shock would be milder, generating asymmetric fluctuations. Second, *macroeconomic* volatility is countercyclical. During expansions uncertainty and overreaction are low while in recessions agents overreact more to economy-wide shocks.

State-dependent overreaction also implies that micro-level volatility is countercyclical:

Proposition 10 The cross-sectional variance of hours worked is given by

$$\int_0^1 \left(\widehat{h}_{i,t}^{\theta} - \widehat{H}_t^{\theta}\right)^2 di = \left[\frac{(1 + \widetilde{\theta}_{t,t-J})(1 - \gamma)}{\eta + (1 + \widetilde{\theta}_{t,t-J})\gamma}\right]^2 \sigma_s^2,$$

and is increasing in $\widetilde{\theta}_{t,t-J}$ and, thus, in the volatility $\sigma_{a,t}^2$ of the idiosyncratic TFP. The cross-sectional variances of output $y_{i,t}$ and consumption $c_{i,t}$ are similarly increasing in the volatility $\sigma_{a,t-1}^2$ of the idiosyncratic TFP.

Proof. See Appendix.

As uncertainty increases, the overreactions to the predictable component of idiosyncratic TFP and the future benefit of labor, captured in the $\left[\frac{(1+\tilde{\theta}_{t,t-J})(1-\gamma)}{\eta+(1+\tilde{\theta}_{t,t-J})\gamma}\right]^2$ term, rise. Hence, an increase in uncertainty about idiosyncratic TFP raises the cross-sectional variances of individual actions.

Our theory has an important policy implication. As we saw above, the micro-level volatility and macroeconomic volatility are tightly linked through the state-dependent overreaction controlled by $\tilde{\theta}_{t,t-J}$. Thus, a policy that reduces microeconomic uncertainty through, for instance, a redistributive tax policy can also be effective in stabilizing the macroeconomy. To fix ideas, consider a progressive income tax and subsidy scheme where the individual rate $\tau_{i,t}$ is increasing in the realized idiosyncratic productivity level:

$$\tau_{i,t} = \tau a_{i,t},$$

where $\tau \geq 0$ is a parameter that controls the progressivity. The island resource constraint is

$$c_{i,t} + \tau_{i,t} y_{i,t} = y_{i,t},$$

so the agent pays a tax $(\tau_{i,t} > 0)$ if the realized TFP shock is positive $(a_{i,t} > 0)$ and receives a transfer $(\tau_{i,t} < 0)$ otherwise. The scheme is budget neutral (up to a first-order approximation).

Proposition 11 A higher progressivity τ is associated with a smaller increase in the effective diagnosticity parameter $\widetilde{\theta}_{t,t-J}$ when the volatility $\sigma_{a,t}^2$ of idiosyncratic TFP rises.

Proof. See Appendix.

Intuitively, redistribution dampens the state-dependent overreaction by reducing cross-sectional uncertainty about the future benefit of labor. Thus, the government can stabilize the macroeconomy by using the tax policy to reduce the increase in uncertainty and overreaction. For instance, in times of low aggregate TFP and high uncertainty, the government can implement the tax policy or increase its progressivity. These interventions would dampen the overreaction and make the downturn less severe.

4.4 Calibrated example

We illustrate the quantitative potential of the Smooth DE mechanism in the context of the parsimonious RBC model presented above by examining its dynamics.

Calibration. We calibrate the model to a quarterly frequency. We set the discount factor $\beta = 0.99$, the IES $\gamma^{-1} = 0.25^{-1}$, and $\eta = 0.4$, which implies a Frisch elasticity of labor supply of 2.5.¹¹ For the economy-wide TFP shock, we set $\rho_A = 0.95$ and $\sigma_A = 0.7/100$. The calibration satisfies the condition $\gamma^{-1} > 1$, so labor increases in response to an increase in expected TFP.

Consider the time-varying standard deviation $\sigma_{a,t}$ of the idiosyncratic TFP shocks. Using Census micro data, Bloom et al. (2018) and Ilut et al. (2018) find that, during recessions, the dispersion of TFP shocks increases by 13% and 7%, respectively. Motivated by these findings, we assume that a larger-than-or-equal-to- one-standard-deviation negative economy-wide TFP innovation is associated with a 10% increase in the standard deviation $\sigma_{a,t}$ of the idiosyncratic TFP shocks relative to the steady-state standard deviation σ_a . Conversely, a larger-than-or-equal-to- one-standard-deviation positive economy-wide TFP innovation is associated with a 10% decrease in the standard deviation $\sigma_{a,t}$.

We assume that the agent's comparison group is the expectation formed J=5 periods ago. The parameter J mainly determines the persistence of overreaction and the value is consistent with Bianchi et al. (2024), who find that in an estimated structural model the memory weights center around five- and six-quarters-ago expectations.

There are three remaining parameters: the steady-state standard deviation of the unpredictable component of the idiosyncratic TFP shock σ_a , the standard deviation of the predictable component of the idiosyncratic TFP shock σ_s , and the diagnosticity parameter θ . We calibrate these parameters so that the model matches the three empirical moments

¹¹These values of IES and Frisch elasticity allow us to generate realistic labor volatility. Our calibrated model generates the time-series standard deviation of aggregate hours worked of 1.67%. In the data, the standard deviation of total hours worked in the nonfarm business sector (1983:Q1–2019:Q4) is 1.66%.

Table 1: Internally calibrated parameters and targeted moments

Parameters		Targeted moments			
			Data	Model	
σ_a	0.022	Realized absolute forecast error	0.143	0.143	
$\dfrac{\sigma_s}{\widetilde{ heta}}$	0.027	Residual uncertainty	0.41	0.41	
$\widetilde{ heta}$	1.547	Skewness of aggregate hours	-0.21	-0.21	

Notes: The table reports the parameters and their calibrated values as well as the targeted moments. σ_a is the steady-state standard deviation of unpredictable component of the idiosyncratic TFP shock, σ_s is the standard deviation of the predictable component of the idiosyncratic TFP shock, and $\tilde{\theta}$ is the long-run average effective diagnosticity implied by the calibrated value of θ . The realized absolute forecast error is reported in Barrero (2022) using survey data on US managers, calculated from realized forecast errors of sales growth between t to t+4, with observations employment-weighted. The residual uncertainty from David et al. (2016) captures the amount of posterior uncertainty relative to the ex-ante uncertainty. The skewness of aggregate hours is calculated using total hours worked in the nonfarm business sector (1983:Q1-2019:Q4). The model moments are calculated using simulated data from the Smooth DE model.

summarized in Table 1.¹² While multiple model parameters jointly affect these moments, we select the moments so that each moment is informative about a parameter of interest.

The first empirical moment, the mean of realized absolute forecast errors, is from Barrero (2022) who uses survey data (Atlanta Fed / Chicago-Booth / Stanford Survey of Business Uncertainty (SBU)) on US managers. Forecast errors are computed by subtracting realized sales growth between t to t+4 from managers' forecasts. The model counterpart is obtained by calculating the mean absolute forecast error on the simulated distribution of the realized forecast error $\mathbb{E}^{\theta}_{i,t} \left[\widehat{y}_{i,t+4}^{RE} \right] - \widehat{y}_{i,t+4}^{\theta}$. This moment is informative about the steady-state standard deviation of the unpredictable component of idiosyncratic TFP.

The second moment, residual uncertainty, captures the amount of posterior uncertainty relative to the ex-ante uncertainty. David et al. (2016) estimate the residual uncertainty to be 41%. The model counterpart is given by $\sigma_a^2/(\sigma_s^2 + \sigma_a^2)$. This moment is useful to pin down the standard deviation σ_s of the predictable component of idiosyncratic TFP.

Finally, the third moment is the skewness of total hours worked in the nonfarm business sector (1983:Q1-2019:Q4).¹⁴ The negative skewness (-0.21) reflects macroeconomic

 $^{^{12}}$ We choose the parameters so that the squared-sum of distance between the data moments and the model-implied moments is minimized.

¹³Specifically, we generate 100 replications of T = 200 time series with n = 500 islands. The number of islands roughly matches the number of firms surveyed in the SBU data in Barrero (2022).

 $^{^{14}}$ The empirical skewness of hours increases significantly to -1.75 when we extend the sample until 2022:Q1 to include the 2020 Covid-19 recession. We use the simulated data to compute the skewness of aggregate

Table 2: Untargeted survey moments: overreaction and overconfidence

	(1)	(2)	(3)	(4)
	$F_t(\Delta y_{i,t+4 t}) - \Delta y_{i,t+4 t}$	Absolute forecast error		
	on $\Delta y_{i,t t-1}$	Realized	Subjective	(Subjective)/(Realized)
Data	0.173	0.143	0.023	0.16
	(0.059)	(0.012)	(0.002)	
Model	0.095	0.143	0.017	0.12

Notes: The table reports the coefficient on overextrapolation and realized and subjective mean absolute forecast errors. The data moments are computed by Barrero (2022) using survey data on US managers, with observations employment-weighted and standard errors in parentheses. The first column reports the coefficient from a panel regression where managers' time t forecast of t+4 sales growth minus the realization is regressed on the sales growth between quarter t-1 to t. The second column is the realized mean absolute forecast error, calculated using realized forecast errors of sales growth between t to t+4. The realized mean absolute forecast error is used in the calibration as a target, but is included in this table to facilitate comparison. The third column is the subjective mean absolute forecast error, where the hypothetical realizations are drawn from managers' subjective probability distributions. The fourth column is the ratio of the subjective absolute forecast error to the realized error. The model moments are calculated using the simulated data from the Smooth DE model.

asymmetry: drops in hours worked are steeper than increases. In our model, a negative economy-wide TFP innovation increases uncertainty $\sigma_{a,t}^2$ and, in turn, the effective overreaction $\widetilde{\theta}_{t,t-J}$. A positive TFP innovation, in contrast, reduces overreaction. Under Smooth DE, the diagnosticity parameter θ governs the strength of this mechanism to generate asymmetry. Under RE model and the standard DE model where the overreaction is constant, there is no asymmetry, and the skewness is zero.

The model moments match the empirical moments perfectly. The calibrated σ_a and σ_s imply the predictable and unpredictable components' variances are about the same in steady state. The long-run average effective diagnosticity parameter $\tilde{\theta}$, implied by the calibrated value of θ , is 1.54. This value is somewhat larger than Bordalo et al. (2018), Bordalo et al. (2019), and d'Arienzo (2020), which tend to estimate the diagnosticity parameter (under standard DE) around 1 but smaller than the estimate of 1.97 in Bianchi et al. (2024).¹⁵

Implications for untargeted survey moments. We examine to what extent our theory can explain untargeted survey evidence on overreaction and overconfidence. We use

hours worked in the model. Both simulated and actual time series are HP-filtered with $\lambda = 1600$.

¹⁵Like Bianchi et al. (2024), our current model features distant memory (J > 1). Bianchi et al. (2024) notes that existing estimates are based primarily on models where imperfect memory is assumed to be driven only by the immediate past (J = 1), and this assumption changes inference about the diagnosticity parameter.

Barrero (2022)'s survey moments as an external validation because the study shows both overreaction and overconfidence based on a single dataset (SBU). The first column of Table 2 reports the coefficient from a panel regression where managers' time t forecast of t+4 sales growth minus the realization is regressed on the sales growth between quarter t-1 to t. The coefficient is positive, meaning that managers' forecasts tend to be excessively optimistic during high growth period: managers overextrapolate. The second column is the realized mean absolute forecast error, reported in Table 1, and is shown here again to facilitate comparison. The third column is the subjective mean absolute forecast error, where the hypothetical realizations are drawn from the managers' subjective probability distributions. The subjective absolute forecast error is only 16% the size of the empirical errors (fourth column), indicating overconfidence: managers overestimate the precision of their forecasts.

The model moments are computed by simulating the model under Smooth DE. First, consider the overextrapolation regression coefficient. The model counterpart is the coefficient on pooled OLS where we regress the Smooth DE four-quarters-ahead forecast error, $\mathbb{E}^{\theta}_{i,t}\left[\widehat{y}^{RE}_{i,t+4}\right] - \widehat{y}^{\theta}_{i,t+4}$, on output growth, $\left[\widehat{y}^{\theta}_{i,t} - \widehat{y}^{\theta}_{i,t-1}\right]$, which proxies for news. The coefficient is positive, but smaller than in the data. The reason why the calibrated model understates this coefficient relative to the data is as follows. In our model, economy-wide shocks are persistent while island-specific shocks are i.i.d. In contrast to persistent shocks, when shocks are i.i.d., the Smooth DE forecasts are orthogonal to news, so the idiosyncratic shocks push the coefficient toward zero. While we specified idiosyncratic TFP shocks to be i.i.d. for tractability, allowing for persistence would increase the overextrapolation coefficient. Thus, our model provides a conservative lower bound on the macroeconomic effects of Smooth DE.

Next, consider the mean absolute forecast errors. The subjective error (third column) is obtained first by calculating the Smooth DE variance of output growth

$$\mathbb{V}_{i,t}^{\theta} \left[\widehat{y}_{i,t+4}^{RE} \right] = \frac{\mathbb{V}_{i,t} \left[\widehat{y}_{i,t+4}^{RE} \right]}{1 + \left(1 - R_{t+1|t,t-J} \right) \theta}, \tag{38}$$

and then leverage the normality of the RE output growth so that the subjective absolute forecast error is given by $\sqrt{2/\pi} \left(\mathbb{V}_{i,t}^{\theta}\left[\widehat{y}_{i,t+4}^{RE}\right]\right)^{\frac{1}{2}}$. The model closely matches the subjective forecast error. The size of the absolute subjective error is 12% of the size of the realized forecast error (fourth column), in line with the survey data's 16%. According to (38), the Smooth DE variance $\mathbb{V}_{i,t}^{\theta}\left[\widehat{y}_{i,t+4}^{RE}\right]$ would be lower than the econometrician's variance $\mathbb{V}_{i,t}\left[\widehat{y}_{i,t+4}^{\theta}\right]$ due to two factors. The first factor is that, under $na\ddot{v}vet\acute{e}$, (Smooth) DE agents perceive future output to follow the RE law of motion $\widehat{y}_{i,t+4}^{RE}$ instead of the equilibrium law of motion $\widehat{y}_{i,t+4}^{\theta}$.

 $^{^{16}}$ This need not be the case when agents forecast endogenous variables in models with slow-moving endogenous states, such as capital. See Bianchi et al. (2024) for details.

Table 3: Countercyclical cross-sectional standard deviation of labor growth

	(1)	(2)	(3)	(4)
	Data	Smooth DE	DE	RE
(Recessions)/(Expansions)	1.16	1.12	1	1

Notes: The table reports the ratio of the cross-sectional standard deviation of labor growth during recessions to the cross-sectional standard deviation during expansions. The first column shows the ratio in the data, reported by Ilut et al. (2018), where recessions and expansions are defined as NBER recessions and NBER expansions, respectively. The second, third, and fourth columns report the model-implied ratios for the Smooth DE, DE, and RE models, respectively.

The second factor is the Smooth DE effect (the denominator in (38)) on uncertainty, according to which a reduction of uncertainty contributes to overconfidence about the precision of expectations. To disentangle these two factors, we calculate the subjective mean absolute forecast error without the Smooth DE effect. We obtain $\sqrt{2/\pi} \left(\mathbb{V}_{i,t} \left[\hat{y}_{i,t+4}^{RE} \right] \right)^{\frac{1}{2}} = 0.053$, which is 37% of the size of the realized errors. This ratio is more than double the values recovered by the data (16%) and implied by the baseline model (12%). We conclude that the Smooth DE effect is important to account for overconfidence as observed in survey data.

Countercyclical micro and macro volatility. We now study the model's ability to generate countercyclical micro and macro volatility. First, consider the micro volatility. In Table 3, we report the ratio of the cross-sectional standard deviation of labor growth during recessions to the cross-sectional standard deviation during expansions. The first column shows this ratio from the data, as reported by Ilut et al. (2018), where recessions and expansions are defined as NBER recessions and NBER expansions, respectively. The crosssectional dispersion is countercyclical: in recessions, it is 16% higher than during expansions. The second column reports the ratio in our model, where we define recessions and expansions as periods when there are one-standard-deviation negative and positive innovations to the economy-wide TFP, respectively. Under Smooth DE the cross-sectional standard deviation of labor growth is 12% higher during recessions than in expansions, so the model explains 75% of the empirical countercyclicality of micro volatility. In the model, a negative aggregate TFP innovation triggers an increase in idiosyncratic TFP uncertainty $\sigma_{a,t}$. As a result, the overreaction $\widetilde{\theta}_{t,t-J}$ to the predictable component $s_{i,t}$ of idiosyncratic TFP rises, so the crosssectional dispersion of actions such as labor increases. As shown in the third and the fourth columns, the cross-sectional dispersion is constant over the business cycle under the standard DE model, where the overreaction is constant, and the RE model, where we have $\theta = 0$.

Next, consider macro volatility. In our model, in times of low TFP and high idiosyncratic

Table 4: Countercyclical volatility of aggregate labor growth

	(1)	(2)	(3)	(4)
	Data	Smooth DE	DE	RE
(Recessions)/(Expansions)	1.23	1.22	1	1

Notes: The table reports the ratio of the rolling standard deviation of aggregate labor growth during recessions to the rolling standard deviation during expansions. The first column shows the ratio in the data for the period 1983:Q1-2019:Q4, where recessions and expansions are defined as NBER recessions and NBER expansions, respectively. The second, third, and fourth columns report the model-implied ratios for the Smooth DE, DE, and RE models, respectively.

uncertainty $\sigma_{a,t}$, aggregate labor responds more to economy-wide shocks because the overreaction is stronger. Table 4 examines to what extent this countercyclical macro volatility is consistent with data. To measure time-varying volatility of aggregate hours worked in data, similar to Ilut et al. (2018), we compute the rolling window standard deviation as

$$\sigma_{H,t} = \sqrt{\frac{1}{n_w - 1} \sum_{k = -(n_w - 1)/2}^{(n_w - 1)/2} \left(\Delta \ln H_{t+k} - \overline{\Delta \ln H_t}\right)^2},$$
(39)

where $\Delta \ln H_{t+k}$ is the log change of total hours worked in the nonfarm business sector from a quarter t+k-1 to t+k and $\overline{\Delta \ln H_t} \equiv (1/n_w) \sum_{k=-(n_w-1)/2}^{(n_w-1)/2} \Delta \ln H_{t+k}$. We set the window size $n_w=3$ and consider the sample 1983:Q1-2019:Q4. The first column of Table 4 reports the measured $\sigma_{H,t}$ during NBER recessions relative to $\sigma_{H,t}$ during NBER expansions. The measured volatility of aggregate labor growth is 23% higher in recessions than in expansions. We then compute the same rolling standard deviation (39) on the simulated data from the model. We define recessions and expansions as periods when there are larger-than-or-equal-to one-standard-deviation negative and positive innovations to the economy-wide TFP, respectively. The second column shows that in the Smooth DE model, the aggregate labor growth volatility $\sigma_{H,t}$ is 22% higher in recessions than in expansions. Thus, the Smooth DE model generates the countercyclical macro volatility that is quantitatively in line with the data, even though the volatility of economy-wide shocks is constant. DE and RE models, in contrast, do not generate such countercyclical volatility (third and fourth columns).

Perceived vs. actual increase in uncertainty. Discussions of Corollary 1 and Figure 3 indicate that, in our model, agents would overestimate the increase in uncertainty in recessions. This is because tail events become more representative when uncertainty rises. To quantify how much the agent's perceived uncertainty rises relative to the actual uncertainty,

we compute the Smooth DE variance of the future marginal benefit of labor,

$$\mathbb{V}_{i,t}^{\theta} \left(-\gamma \widehat{c}_{i,t+1}^{RE} + A_{t+1} + a_{i,t+1} \right) = \frac{\mathbb{V}_{i,t} \left(-\gamma \widehat{c}_{i,t+1}^{RE} + A_{t+1} + a_{i,t+1} \right)}{1 + \theta (1 - R_{t+1|t,t-J})}.$$
 (40)

We are interested in (40) because it controls the labor-supply decision in response to an uncertainty increase. We find that, under our calibration, a 10% rise in $\sigma_{a,t}$ raises the perceived uncertainty (40) by 69%. In contrast, actual uncertainty, given by $V_{i,t} \left(-\gamma \hat{c}_{i,t+1}^{\theta} + A_{t+1} + a_{i,t+1}\right)$ rises only by 19%. Thus, the perceived rise in uncertainty is more than three times larger than the actual uncertainty increase in recessions.¹⁷

5 Conclusions

We developed a tractable and structural bridge from the representativeness heuristic of Kahneman and Tversky (1972) to the time-series domain. We built on the formalization of representativeness by Gennaioli and Shleifer (2010) and of diagnostic expectations (DE) by Bordalo et al. (2018) to allow for what we call "smooth diagnosticity." Under Smooth DE new information is defined as the difference between the current information set and a previous information set. A critical consequence of this basic approach is that current and past uncertainty interact to determine the intensity of the DE overreaction, but also create the preconditions for novel properties such as over- and under- confidence.

After formally characterizing Smooth DE and its key properties, we leveraged its insights along two substantive directions. First, we embedded the Smooth DE framework in a standard signal extraction problem and showed that Smooth DE can account for recent evidence indicating that overreaction is stronger for weaker signals and for longer horizon forecasts. Second, we embedded Smooth DE in a parsimonious RBC model with time-varying uncertainty. This model can account for survey data on overreaction and overconfidence as well as three salient properties of the business cycle: (1) asymmetry, (2) countercyclical micro volatility, and (3) countercyclical macro volatility. We uncovered a novel policy implication: a redistributive policy that reduces idiosyncratic uncertainty could be beneficial for macroeconomic stabilization because it dampens the state-dependent overreaction.

¹⁷Since we linearize our model, the increase in uncertainty affects first-order economic outcomes through the state-dependent overreaction and not through the conventional risk channel. The risk adjusted log-linearization method as in Bianchi et al. (2023) would allow us to capture the impact of perceived increase in uncertainty while preserving tractability.

References

- Altig, D., J. M. Barrero, N. Bloom, S. J. Davis, B. Meyer, and N. Parker (2020). Surveying business uncertainty. *Journal of Econometrics*.
- Augenblick, N., E. Lazarus, and M. Thaler (2021). Overinference from weak signals and underinference from strong signals.
- Barberis, N. (2018). Psychology-based models of asset prices and trading volume. In *Hand-book of behavioral economics: applications and foundations 1*, Volume 1, pp. 79–175.
- Barrero, J. M. (2022). The micro and macro of managerial beliefs. *Journal of Financial Economics* 143(2), 640–667.
- Basu, S. and B. Bundick (2017). Uncertainty shocks in a model of effective demand. *Econometrica* 85, 937–958.
- Bianchi, F., C. Ilut, and H. Saijo (2024). Diagnostic business cycles. *The Review of Economic Studies* 91(1), 129–162.
- Bianchi, F., H. Kung, and M. Tirskikh (2023, July). The origins and effects of macroeconomic uncertainty. *Quantitative Economics* 14(3), 855–896.
- Bloom, N. (2009). The impact of uncertainty shocks. Econometrica 77(3), 623–685.
- Bloom, N., M. Floetotto, N. Jaimovich, I. Saporta-Eksten, and S. J. Terry (2018, May). Really uncertain business cycles. *Econometrica* 86(3), 1031–1065.
- Bordalo, P., K. Coffman, N. Gennaioli, F. Schwerter, and A. Shleifer (2020). Memory and representativeness. *Psychological Review*. forthcoming.
- Bordalo, P., N. Gennaioli, R. La Porta, M. OBrien, and A. Shleifer (2023). Long term expectations and aggregate fluctuations. *NBER Macro Annual*.
- Bordalo, P., N. Gennaioli, Y. Ma, and A. Shleifer (2020). Overreaction in macroeconomic expectations. *American Economic Review* 110(9), 2748–82.
- Bordalo, P., N. Gennaioli, R. L. Porta, and A. Shleifer (2019). Diagnostic expectations and stock returns. *The Journal of Finance* 74(6), 2839–2874.
- Bordalo, P., N. Gennaioli, and A. Shleifer (2018). Diagnostic expectations and credit cycles. The Journal of Finance 73(1), 199–227.

- Bordalo, P., N. Gennaioli, and A. Shleifer (2022). Overreaction and diagnostic expectations in macroeconomics. *Journal of Economic Perspectives* 36(3), 223–44.
- Bordalo, P., N. Gennaioli, A. Shleifer, and S. J. Terry (2019). Real credit cycles. Harvard, mimeo.
- Born, B., Z. Enders, M. Menkhoff, G. J. Müller, and K. Niemann (2022). Firm expectations and news: Micro v macro. Technical report, mimeo.
- Born, B., Z. Enders, G. J. Müller, and K. Niemann (2022). Firm expectations about production and prices: Facts, determinants, and effects. *Handbook of Economic Expectations*.
- Daniel, K., D. Hirshleifer, and A. Subrahmanyam (1998). Investor psychology and security market under-and overreactions. *The Journal of Finance* 53(6), 1839–1885.
- Daniel, K. D., D. Hirshleifer, and A. Subrahmanyam (2001). Overconfidence, arbitrage, and equilibrium asset pricing. *The Journal of Finance* 56(3), 921–965.
- d'Arienzo, D. (2020). Maturity increasing overreaction and bond market puzzles. Bocconi University, Working Paper.
- David, J. M., H. A. Hopenhayn, and V. Venkateswaran (2016). Information, misallocation, and aggregate productivity. *Quarterly Journal of Economics* 131(2), 943—1005.
- De Bondt, W. F. and R. H. Thaler (1995). Financial decision-making in markets and firms: A behavioral perspective. *Handbooks in operations research and management science* 9, 385–410.
- Fernández-Villaverde, J., P. Guerrón-Quintana, K. Kuester, and J. F. Rubio-Ramírez (2015). Fiscal volatility shocks and economic activity. *American Economic Review* 105(11), 3352–3384.
- Fernández-Villaverde, J., P. Guerrón-Quintana, J. F. Rubio-Ramírez, and M. Uribe (2011). Risk matters: The real effects of volatility shocks. *American Economic Review* 101(6), 2530–2561.
- Gennaioli, N. and A. Shleifer (2010). What comes to mind. The Quarterly Journal of Economics 125(4), 1399–1433.
- Hamilton, J. D. (1989). A new approach to the economic analysis of nonstationary time series and the business cycle. *Econometrica* 57(2), 357–384.

- Ilut, C. L., M. Kehrig, and M. Schneider (2018, September). Slow to hire, quick to fire: Employment dynamics with asymmetric responses to news. *Journal of Political Economy* 126(5), 2011–2071.
- Jurado, K., S. C. Ludvigson, and S. Ng (2015, March). Measuring uncertainty. *American Economic Review* 105(3), 1177–1216.
- Kahneman, D. and A. Tversky (1972). Subjective probability: A judgment of representativeness. *Cognitive psychology* 3(3), 430–454.
- Kreps, D. (1998). Anticipated utility and dynamic choice. In D. P. Jacobs, E. Kalai, and M. I. Kamien (Eds.), Frontiers of Research in Economic Theory. Cambridge University Press.
- Lucas, R. E. (1976). Econometric policy evaluation: A critique. In *Carnegie-Rochester* conference series on public policy, Volume 1, pp. 19–46.
- McKay, A. and R. Reis (2008). The brevity and violence of contractions and expansions. Journal of Monetary Economics 55(4), 738–751.
- Morley, J. and J. Piger (2012). The asymmetric business cycle. Review of Economics and Statistics 94(1), 208–221.
- Neftci, S. N. (1984). Are economic time series asymmetric over the business cycle? *Journal of Political Economy*, 556–569.
- O'Donoghue, T. and M. Rabin (1999). Doing it now or later. American Economic Review 89(1), 103–124.
- Sichel, D. F. (1993). Business cycle asymmetry: A deeper look. *Economic Inquiry* 31(2), 224–236.
- Woodford, M. (2001). Imperfect common knowledge and the effects of monetary policy. NBER Working Paper 8673.

A Proofs

A.1 Proof of Proposition 1

Expression (2) can be written as:

$$h_t^{\theta}(\widehat{\omega}_{t+1}) \propto \exp\left[-\frac{1}{2\sigma_{t+h|t}^2} \left(\omega_{t+1} - \mu_{t+1|t}\right)^2\right] \left[\frac{\exp\left[-\frac{1}{2\sigma_{t+1|t}^2} \left(\omega_{t+1} - \mu_{t+1|t}\right)^2\right]}{\exp\left[-\frac{1}{2\sigma_{t+1|t-J}^2} \left(\omega_{t+1} - \mu_{t+1|t-J}\right)^2\right]}\right]^{\theta} \frac{1}{Z}$$

Collecting the terms in the exponents, we get:

$$h_t^{\theta}(\widehat{\omega}_{t+1}) \propto \exp\left[-\frac{1}{2\sigma_{t+1|t}^2} \left[(1+\theta) \left(\omega_{t+1} - \mu_{t+1|t}\right)^2 - \frac{\sigma_{t+1|t}^2}{\sigma_{t+1|t-J}^2} \theta \left(\omega_{t+1} - \mu_{t+1|t-J}\right)^2 \right] \right] \frac{1}{Z}$$

Developing the squared terms and keeping track of the terms involving ω_{t+1} , we obtain:

$$h_{t}^{\theta}\left(\widehat{\omega}_{t+1}\right) \propto \exp \left[\begin{array}{c} -\frac{1}{2\sigma_{t+1|t}^{2}} \left(1 + \theta - \frac{\sigma_{t+1|t}^{2}}{\sigma_{t+1|t-J}^{2}} \theta\right) \\ \left[\omega_{t+1}^{2} - 2\omega_{t+1} \left(1 + \theta - \frac{\sigma_{t+1|t}^{2}}{\sigma_{t+1|t-J}^{2}} \theta\right)^{-1} \left(\mu_{t+1|t} \left(1 + \theta\right) - \frac{\sigma_{t+1|t}^{2}}{\sigma_{t+1|t-J}^{2}} \theta \mu_{t+1|t-J}\right) \right] \right] \frac{1}{Z} dt$$

where the remaining terms are absorbed in the constant of integration.

Define: $R_{t+1|t,t-J} \equiv \frac{\sigma_{t+1|t}^2}{\sigma_{t+1|t-J}^2}$. If $R_{t+1|t,t-J} > (1+\theta)/\theta$, the expression above corresponds to the kernel of a normal with mean:

$$\mathbb{E}_{t}^{\theta}\left(\omega_{t+1}\right) = \left(1 + \theta - \frac{\sigma_{t+1|t}^{2}}{\sigma_{t+1|t-J}^{2}}\theta\right)^{-1} \left[\mu_{t+1|t}\left(1 + \theta\right) - \frac{\sigma_{t+1|t}^{2}}{\sigma_{t+1|t-J}^{2}}\theta\mu_{t+1|t-J}\right]$$

$$= \left[\mu_{t+1|t} + \frac{R_{t+1|t,t-J}\theta}{1 + \left(1 - R_{t+1|t,t-J}\right)\theta}\left(\mu_{t+1|t} - \mu_{t+1|t-J}\right)\right]$$

and variance:

$$\mathbb{V}_{t}^{\theta}(\omega_{t+1}) = \sigma_{t+1|t}^{2} \left(1 + \theta - \frac{\sigma_{t+1|t}^{2}}{\sigma_{t+1|t-J}^{2}} \theta \right)^{-1}$$
$$= \frac{\sigma_{t+1|t}^{2}}{1 + \left(1 - R_{t+1|t,t-J} \right) \theta}.$$

This gives us the result stated in Proposition 2.

A.2 Proof of Proposition 3

Re-writing the expression (20):

$$h_t^{\theta}(x_t) \propto \exp\left[-\frac{1}{2\Sigma_{t|t}} (x_t - \tilde{x}_{t|t})^2\right] \left[\frac{\exp\left[-\frac{1}{2\Sigma_{t|t}} (x_t - \tilde{x}_{t|t})^2\right]}{\exp\left[-\frac{1}{2\Sigma_{t|t-1}} (x_t - \tilde{x}_{t|t-1})^2\right]}\right]^{\theta} \frac{1}{Z}$$

Collecting the terms in the exponents, we get:

$$h_t^{\theta}\left(x_t\right) \propto \exp\left[-\frac{1}{2\Sigma_{t|t}}\left[\left(1+\theta\right)\left(x_t-\tilde{x}_{t|t}\right)^2 - \frac{\Sigma_{t|t}}{\Sigma_{t|t-1}}\theta\left(x_t-\tilde{x}_{t|t-1}\right)^2\right]\right]\frac{1}{Z}$$

Developing the squared terms and keeping track of the terms involving x_t , we obtain:

$$h_t^{\theta}\left(x_t\right) \propto \exp \left[\begin{array}{c} -\frac{1}{2\Sigma_{t|t}} \left(1 + \theta - \frac{\Sigma_{t|t}}{\Sigma_{t|t-1}} \theta\right) \\ \left[x_t^2 - 2x_t \left(1 + \theta - \frac{\Sigma_{t|t}}{\Sigma_{t|t-1}} \theta\right)^{-1} \left(\left(1 + \theta\right) \tilde{x}_{t|t} - \frac{\Sigma_{t|t}}{\Sigma_{t|t-1}} \theta \tilde{x}_{t|t-1}\right) \right] \right] \frac{1}{Z}$$

where the remaining terms are absorbed in the constant of integration. The one above is the kernel of a normal with mean:

$$\mathbb{E}_{t}^{\theta}(x_{t}) = \left(1 + \theta - \frac{\sum_{t|t}}{\sum_{t|t-1}}\theta\right)^{-1} \left((1+\theta)\,\tilde{x}_{t|t} - \frac{\sum_{t|t}}{\sum_{t|t-1}}\theta\tilde{x}_{t|t-1}\right)$$

$$= \tilde{x}_{t|t} + \frac{R_{t|t,t-1}\theta}{1 + \left(1 - R_{t|t,t-1}\right)\theta} \left(\tilde{x}_{t|t} - \tilde{x}_{t|t-1}\right)$$

$$= \tilde{x}_{t|t-1} + \left(1 + \frac{R_{t|t,t-1}\theta}{1 + \left(1 - R_{t|t,t-1}\right)\theta}\right) \left(\tilde{x}_{t|t} - \tilde{x}_{t|t-1}\right)$$

$$= \tilde{x}_{t|t-1} + \left(1 + \frac{R_{t|t,t-1}\theta}{1 + \left(1 - R_{t|t,t-1}\right)\theta}\right) K_{t}(s_{t} - \tilde{x}_{t|t-1}),$$

where $R_{t|t,t-1} \equiv \Sigma_{t|t}/\Sigma_{t|t-1}$ and in the fourth line we used (2.7.2), and variance:

$$\mathbb{V}_{t}^{\theta}\left(x_{t}\right) = \Sigma_{t|t} \left(1 + \theta - \frac{\Sigma_{t|t}}{\Sigma_{t|t-1}}\theta\right)^{-1}$$
$$= \frac{\Sigma_{t|t}}{1 + \left(1 - R_{t|t,t-1}\right)\theta}.$$

This gives us the result stated in Proposition 3.

A.3 Proof of Proposition 5

First, consider the inequality (27). We have

$$\frac{\partial \mathbb{E}^{\theta} (x_{t} | s_{W,t})}{\partial s_{W,t}^{*}} - \frac{\partial \mathbb{E}^{*} (x_{t} | s_{W,t}^{*})}{\partial s_{W,t}^{*}} = \left[1 + \frac{\theta (1 - K_{W})}{1 + \theta K_{W}} \right] K_{W} - K_{W}^{*}$$

$$= \frac{(1 + \theta)K_{W}}{1 + \theta K_{W}} - K_{W}^{*}$$

$$= \left[\frac{(1 + \theta)K_{W}}{K_{W}^{*}} - (1 + \theta K_{W}) \right] \frac{K_{W}^{*}}{1 + \theta K_{W}}$$

$$= \left[\frac{(1 + \theta)(\sigma_{x}^{2} + \sigma_{W}^{2})}{\sigma_{x}^{2} + \sigma_{\varepsilon,c}^{2}} - \left(1 + \theta \frac{\sigma_{x}^{2}}{\sigma_{x}^{2} + \sigma_{W}^{2} + \sigma_{\varepsilon,c}^{2}} \right) \right] \frac{K_{W}^{*}}{1 + \theta K_{W}}$$

$$= \left[\theta \sigma_{W}^{2} - \sigma_{\varepsilon,c}^{2} \right] \frac{K_{W}^{*}}{1 + \theta K_{W}},$$

which is positive if $\sigma_W^2 > \frac{\sigma_{\varepsilon,c}^2}{\theta}$.

Next, consider the inequality (28). We have

$$\frac{\partial \mathbb{E}^{\theta} \left(x_{t} | s_{S,t} \right)}{\partial s_{S,t}^{*}} - \frac{\partial \mathbb{E}^{*} \left(x_{t} | s_{S,t}^{*} \right)}{\partial s_{S,t}^{*}} = \left[1 + \frac{\theta (1 - K_{S})}{1 + \theta K_{S}} \right] K_{S} - K_{S}^{*}$$

$$= \frac{(1 + \theta)K_{S}}{1 + \theta K_{S}} - K_{S}^{*}$$

$$= \left[\frac{(1 + \theta)K_{S}}{K_{S}^{*}} - (1 + \theta K_{S}) \right] \frac{K_{S}^{*}}{1 + \theta K_{S}}$$

$$= \left[\frac{(1 + \theta)(\sigma_{x}^{2} + \sigma_{S}^{2})}{\sigma_{x}^{2} + \sigma_{S}^{2} + \sigma_{\varepsilon,c}^{2}} - \left(1 + \theta \frac{\sigma_{x}^{2}}{\sigma_{x}^{2} + \sigma_{S}^{2} + \sigma_{\varepsilon,c}^{2}} \right) \right] \frac{K_{S}^{*}}{1 + \theta K_{S}}$$

$$= \left[\theta \sigma_{S}^{2} - \sigma_{\varepsilon,c}^{2} \right] \frac{K_{S}^{*}}{1 + \theta K_{S}},$$

which is negative if $\sigma_S^2 < \frac{\sigma_{\varepsilon,c}^2}{\theta}$.

A.4 Proof of Proposition 6

First, consider the equilibrium individual policy functions. To characterize dynamics we use a log-linear approximation of decision rules around the steady state. We take logs of the optimality condition with respect to hours in (31) and constraints (29) and (30):

$$\begin{split} & \eta \widehat{h}_{i,t} = \mathbb{E}_{i,t} \left[-\gamma \widehat{c}_{i,t+1} + \widehat{z}_{i,t+1} \right], \\ & \widehat{y}_{i,t} = \widehat{z}_{i,t} + \widehat{h}_{i,t-1} = \widehat{c}_{i,t}. \end{split}$$

Substitute the constraints into the labor supply condition:

$$\begin{split} \eta \widehat{h}_{i,t} &= \mathbb{E}_{i,t} \left[-\gamma \widehat{c}_{i,t+1} + \widehat{z}_{i,t+1} \right] \\ &= \mathbb{E}_{i,t} \left[-\gamma \left(\widehat{z}_{i,t+1} + \widehat{h}_{i,t} \right) + \widehat{z}_{i,t+1} \right] \\ \widehat{h}_{i,t} &= \frac{1-\gamma}{\eta+\gamma} \mathbb{E}_{i,t} \left[\widehat{z}_{i,t+1} \right] \\ &= \frac{1-\gamma}{\eta+\gamma} \left[\rho_A A_t + \widetilde{a}_{i,t+1|t} \right] \\ &= \frac{1-\gamma}{\eta+\gamma} \left[\rho_A A_t + s_{i,t} \right]. \end{split}$$

Equating the coefficients we obtain the equilibrium elasticities.

Next, consider aggregate variables. Note we have

$$\int_0^1 s_{i,t} di = 0, \quad \int_0^1 \widehat{z}_{i,t} di = A_t + \int_0^1 a_{i,t} di = A_t,$$

by law of large numbers. Then

$$\widehat{H}_{t} = \int_{0}^{1} \widehat{h}_{i,t} di = \varepsilon \rho_{A} A_{t} + \varepsilon \int_{0}^{1} s_{i,t} di$$

$$= \varepsilon \rho_{A} A_{t}$$

$$\widehat{Y}_{t} = \int_{0}^{1} \widehat{y}_{i,t} di = \int_{0}^{1} \widehat{z}_{i,t} di + \int_{0}^{1} \widehat{h}_{i,t-1} di$$

$$= A_{t} + \widehat{H}_{t-1}$$

$$= \widehat{C}_{t}$$

A.5 Proof of Proposition 7

Note we have

$$\int_0^1 s_{i,t}^2 di = \sigma_s^2, \quad \int_0^1 u_{a,i,t}^2 di = \sigma_{a,t-1}^2, \quad \int_0^1 a_{i,t}^2 di = \int_0^1 (s_{i,t-1} + u_{a,i,t})^2 di = \sigma_s^2 + \sigma_{a,t-1}^2.$$

Then

$$\int_0^1 \left(\widehat{h}_{i,t} - \widehat{H}_t\right)^2 di = \int_0^1 \left(\varepsilon s_{i,t}\right)^2 di = \left(\varepsilon\right)^2 \int_0^1 s_{i,t}^2 di$$
$$= \left(\varepsilon\right)^2 \sigma_s^2,$$

which is constant. Next consider the cross-sectional variance of output:

$$\int_{0}^{1} \left(\widehat{y}_{i,t} - \widehat{Y}_{t}\right)^{2} di = \int_{0}^{1} \left(\left(A_{t} + a_{i,t} + \widehat{h}_{i,t-1}\right) - \left(A_{t} + \widehat{H}_{t-1}\right)\right)^{2} di$$

$$= \int_{0}^{1} \left(a_{i,t} + \varepsilon s_{i,t-1}\right)^{2} di$$

$$= \int_{0}^{1} \left(s_{i,t-1} + u_{a,i,t} + \varepsilon s_{i,t-1}\right)^{2} di$$

$$= \left(1 + \varepsilon\right)^{2} \int_{0}^{1} s_{i,t-1}^{2} di + \int_{0}^{1} u_{a,i,t}^{2} di$$

$$= \left(1 + \varepsilon\right)^{2} \sigma_{s}^{2} + \sigma_{a,t-1}^{2},$$

which is increasing in $\sigma_{a,t-1}^2$. It follows that the cross-sectional variance of consumption:

$$\int_0^1 \left(\widehat{c}_{i,t} - \widehat{C}_t\right)^2 di = (1 + \varepsilon)^2 \sigma_s^2 + \sigma_{a,t-1}^2,$$

is increasing in $\sigma_{a,t-1}^2$ as well.

A.6 Proof of Proposition 8

First, consider the equilibrium individual policy functions. As in the RE solution, to characterize dynamics we use a log-linear approximation of decision rules around the steady state. We take logs of the optimality condition with respect to hours in (32) and constraints (29) and (30):

$$\begin{split} & \eta \widehat{h}_{i,t}^{\theta} = \mathbb{E}_{i,t}^{\theta} \left[-\gamma \widehat{c}_{i,t+1}^{RE} + \widehat{z}_{i,t+1} \right] \\ & \widehat{y}_{i,t}^{\theta} = \widehat{z}_{i,t} + \widehat{h}_{i,t-1}^{\theta} = \widehat{c}_{i,t}^{\theta}. \end{split}$$

Substitute the constraints into the labor supply condition:

$$\begin{split} \eta \widehat{h}_{i,t}^{\theta} &= (1 + \widetilde{\theta}_{t,t-J}) \mathbb{E}_{i,t} \left[-\gamma \widehat{c}_{i,t+1}^{RE} + \widehat{z}_{i,t+1} \right] - \widetilde{\theta}_{t,t-J} \mathbb{E}_{i,t-J} \left[-\gamma \widehat{c}_{i,t+1}^{RE} + \widehat{z}_{i,t+1} \right] \\ \eta \widehat{h}_{i,t}^{\theta} &= (1 + \widetilde{\theta}_{t,t-J}) \mathbb{E}_{i,t} \left[-\gamma \left(\widehat{z}_{i,t+1} + \widehat{h}_{i,t}^{\theta} \right) + \widehat{z}_{i,t+1} \right] \\ &- \widetilde{\theta}_{t,t-J} \mathbb{E}_{i,t-J} \left[-\gamma \left(\widehat{z}_{i,t+1} + \widehat{h}_{i,t}^{RE} \right) + \widehat{z}_{i,t+1} \right] \\ \left[\eta + \left(1 + \widetilde{\theta}_{t,t-J} \right) \gamma \right] \widehat{h}_{i,t}^{\theta} &= (1 + \widetilde{\theta}_{t,t-J}) \left(1 - \gamma \right) \mathbb{E}_{i,t} \left[\widehat{z}_{i,t+1} \right] - \widetilde{\theta}_{t,t-J} \left(1 - \gamma \right) \mathbb{E}_{i,t-J} \left[\widehat{z}_{i,t+1} \right] + \widetilde{\theta}_{t,t-J} \gamma \mathbb{E}_{i,t-J} \left[\widehat{h}_{i,t}^{RE} \right] \\ \left[\eta + \left(1 + \widetilde{\theta}_{t,t-J} \right) \gamma \right] \widehat{h}_{i,t}^{\theta} &= (1 + \widetilde{\theta}_{t,t-J}) \left(1 - \gamma \right) \left[\rho_{A} A_{t} + s_{i,t} \right] \\ &- \widetilde{\theta}_{t,t-J} \left(1 - \gamma \right) \rho_{A}^{J+1} A_{t-J} + \widetilde{\theta}_{t,t-J} \gamma \left[\varepsilon \rho_{A}^{J+1} A_{t-J} \right] \\ \widehat{h}_{i,t}^{\theta} &= \frac{\left(1 + \widetilde{\theta}_{t,t-J} \right) \left(1 - \gamma \right)}{\eta + \left(1 + \widetilde{\theta}_{t,t-J} \right) \gamma} \rho_{A} A_{t} + \frac{\left(1 + \widetilde{\theta}_{t,t-J} \right) \left(1 - \gamma \right)}{\eta + \left(1 + \widetilde{\theta}_{t,t-J} \right) \gamma} s_{i,t} \\ &- \frac{\widetilde{\theta}_{t,t-J} \eta}{\eta + \left(1 + \widetilde{\theta}_{t,t-J} \right) \gamma} \left[\frac{1 - \gamma}{\eta + \gamma} \right] \rho_{A}^{J+1} A_{t-J}, \end{split}$$

where the effective diagnosticity parameter $\tilde{\theta}_{t,t-J}$ is given by (35). Equating the coefficients we obtain the equilibrium elasticities. As in the RE economy, we obtain equilibrium aggregate variables by simply aggregating the individual policy functions.

A.7 Proof of Proposition 9

Consider $R_{t+1|t,t-J}$:

$$\begin{split} R_{t+1|t,t-J} &= \frac{\mathbb{V}_{i,t} \left(-\gamma \widehat{c}_{i,t+1}^{RE} + \widehat{z}_{i,t+1} \right)}{\mathbb{V}_{i,t-J} \left(-\gamma \widehat{c}_{i,t+1}^{RE} + \widehat{z}_{i,t+1} \right)} \\ &= \frac{\mathbb{V}_{i,t} \left(-\gamma \left(\widehat{z}_{i,t+1} + \widehat{h}_{i,t}^{\theta} \right) + \widehat{z}_{i,t+1} \right)}{\mathbb{V}_{i,t-J} \left(-\gamma \left(\widehat{z}_{i,t+1} + \widehat{h}_{i,t}^{RE} \right) + \widehat{z}_{i,t+1} \right)} \\ &= \frac{\mathbb{V}_{i,t} \left((1-\gamma) \widehat{z}_{i,t+1} - \gamma \widehat{h}_{i,t}^{\theta} \right)}{\mathbb{V}_{i,t-J} \left((1-\gamma) \widehat{z}_{i,t+1} - \gamma \widehat{h}_{i,t}^{RE} \right)}, \end{split}$$

where the numerator is

$$\mathbb{V}_{i,t}\left((1-\gamma)\left[\rho_{A}A_{t}+u_{A,t+1}+s_{i,t}+u_{a,i,t+1}\right]-\gamma\widehat{h}_{i,t}^{\theta}\right)=\left(1-\gamma\right)^{2}\left(\sigma_{A}^{2}+\sigma_{a,t}^{2}\right),$$

which is increasing in $\sigma_{a,t}^2$. Thus $R_{t+1|t,t-J}$ and in turn $\widetilde{\theta}_{t,t-J}$ are increasing in $\sigma_{a,t}^2$.

A.8 Proof of Proposition 10

First consider the cross-sectional variance of hours. Defining $\varepsilon_{s,t}^{\theta} \equiv \frac{(1+\widetilde{\theta}_{t,t-J})(1-\gamma)}{\eta+(1+\widetilde{\theta}_{t,t-J})\gamma}$, we have

$$\int_{0}^{1} \left(\widehat{h}_{i,t}^{\theta} - \widehat{H}_{t}^{\theta}\right)^{2} di = \int_{0}^{1} \left(\varepsilon_{s,t}^{\theta} s_{i,t}\right)^{2} di = \left(\varepsilon_{s,t}^{\theta}\right)^{2} \int_{0}^{1} s_{i,t}^{2} di$$

$$= \left[\frac{\left(1 + \widetilde{\theta}_{t,t-J}\right) \left(1 - \gamma\right)}{\eta + \left(1 + \widetilde{\theta}_{t,t-J}\right) \gamma}\right]^{2} \sigma_{s}^{2},$$

which is increasing in $\widetilde{\theta}_{t,t-J}$. Next consider the cross-sectional variance of output:

$$\int_{0}^{1} \left(\widehat{y}_{i,t}^{\theta} - \widehat{Y}_{t}^{\theta}\right)^{2} di$$

$$= \int_{0}^{1} \left(\left(A_{t} + a_{i,t} + \widehat{h}_{i,t-1}^{\theta}\right) - \left(A_{t} + \widehat{H}_{t-1}^{\theta}\right)\right)^{2} di$$

$$= \int_{0}^{1} \left(s_{i,t-1} + u_{a,i,t} + \varepsilon_{s,t-1}^{\theta} s_{i,t-1}\right)^{2} di$$

$$= \left(1 + \left[\frac{\left(1 + \widetilde{\theta}_{t,t-J}\right)\left(1 - \gamma\right)}{\eta + \left(1 + \widetilde{\theta}_{t,t-J}\right)\gamma}\right]\right)^{2} \sigma_{s}^{2} + \sigma_{a,t-1}^{2}$$

which is increasing in $\theta_{t,t-J}$ and $\sigma_{a,t-1}^2$. It follows that the cross-sectional variance of consumption:

$$\int_{0}^{1} \left(\widehat{c}_{i,t}^{\theta} - \widehat{C}_{t}^{\theta}\right)^{2} di \left(1 + \left[\frac{\left(1 + \widetilde{\theta}_{t,t-J}\right)\left(1 - \gamma\right)}{\eta + \left(1 + \widetilde{\theta}_{t,t-J}\right)\gamma}\right]\right)^{2} \sigma_{s}^{2} + \sigma_{a,t-1}^{2}$$

is increasing in $\widetilde{\theta}_{t,t-J}$ and $\sigma^2_{a,t-1}$ as well.

A.9 Proof of Proposition 11

First, we solve for the log-linearized RE decision rules under the tax policy. The optimality conditions are

$$\eta \widehat{h}_{i,t} = \mathbb{E}_{i,t} \left[-\gamma \widehat{c}_{i,t+1} + A_{t+1} + (1-\tau) a_{i,t+1} \right]
\widehat{y}_{i,t} = \widehat{z}_{i,t} + \widehat{h}_{i,t-1}
\widehat{c}_{i,t} + \tau a_{i,t} = \widehat{y}_{i,t}.$$

Substitute the constraints into labor supply conditions:

$$\begin{split} \eta \widehat{h}_{i,t} &= \mathbb{E}_{i,t} \left[-\gamma \widehat{c}_{i,t+1} + A_{t+1} + (1-\tau) a_{i,t+1} \right] \\ &= \mathbb{E}_{i,t} \left[-\gamma \left(A_{t+1} + (1-\tau) a_{i,t+1} + \widehat{h}_{i,t} \right) + A_{t+1} + (1-\tau) a_{i,t+1} \right] \\ \widehat{h}_{i,t} &= \frac{1-\gamma}{\eta+\gamma} \mathbb{E}_{i,t} \left[A_{i,t+1} \right] + \frac{1-\gamma}{\eta+\gamma} (1-\tau) \mathbb{E}_{i,t} \left[a_{i,t+1} \right] \\ &= \frac{1-\gamma}{\eta+\gamma} \left[\rho_A A_t + (1-\tau) \widetilde{a}_{i,t+1|t} \right] \\ &= \frac{1-\gamma}{\eta+\gamma} \left[\rho_A A_t + (1-\tau) s_{i,t} \right] \end{split}$$

Equilibrium output and consumption follow immediately as

$$\widehat{y}_{i,t} = \widehat{z}_{i,t} + \widehat{h}_{i,t-1} = A_t + a_{i,t} + \widehat{h}_{i,t-1}, \tag{41}$$

$$\widehat{c}_{i,t} = \widehat{y}_{i,t} - \tau a_{i,t} = A_t + (1 - \tau)a_{i,t} + \widehat{h}_{i,t-1}. \tag{42}$$

Next, consider the log-linearized SDE decision rules under the tax policy. To characterize dynamics we use a log-linear approximation of decision rules around the steady state. The optimality conditions are

$$\eta \widehat{h}_{i,t}^{\theta} = \mathbb{E}_{i,t}^{\theta} \left[-\gamma \widehat{c}_{i,t+1}^{RE} + A_{t+1} + (1-\tau)a_{i,t+1} \right],$$

$$\widehat{y}_{i,t}^{\theta} = \widehat{z}_{i,t} + \widehat{h}_{i,t-1}^{\theta},$$

$$\widehat{c}_{i,t}^{\theta} + \tau a_{i,t} = \widehat{y}_{i,t}^{\theta}.$$

Substitute the constraints into the labor supply condition:

$$\begin{split} \eta \widehat{h}_{i,t}^{\theta} &= (1 + \widetilde{\theta}_{t,t-J}) \mathbb{E}_{i,t} \left[-\gamma \widehat{c}_{i,t+1}^{RE} + A_{t+1} + (1-\tau) a_{i,t+1} \right] - \widetilde{\theta}_{t,t-J} \mathbb{E}_{i,t-J} \left[-\gamma \widehat{c}_{i,t+1}^{RE} + A_{t+1} + (1-\tau) a_{i,t+1} \right] \\ \eta \widehat{h}_{i,t}^{\theta} &= (1 + \widetilde{\theta}_{t,t-J}) \mathbb{E}_{i,t} \left[-\gamma \left(A_{t+1} + (1-\tau) a_{i,t+1} + \widehat{h}_{i,t}^{\theta} \right) + A_{t+1} + (1-\tau) a_{i,t+1} \right] \\ &- \widetilde{\theta}_{t,t-J} \mathbb{E}_{i,t-J} \left[-\gamma \left(A_{t+1} + (1-\tau) a_{i,t+1} + \widehat{h}_{i,t}^{RE} \right) + A_{t+1} + (1-\tau) a_{i,t+1} \right] \\ \left[\eta + \left(1 + \widetilde{\theta}_{t,t-J} \right) \gamma \right] \widehat{h}_{i,t}^{\theta} &= (1 + \widetilde{\theta}_{t,t-J}) (1-\gamma) \mathbb{E}_{i,t} \left[A_{t+1} + (1-\tau) a_{i,t+1} \right] \\ &- \widetilde{\theta}_{t,t-J} \left(1 - \gamma \right) \mathbb{E}_{i,t-J} \left[A_{t+1} + (1-\tau) a_{i,t+1} \right] + \widetilde{\theta}_{t,t-J} \gamma \mathbb{E}_{i,t-J} \left[\widehat{h}_{i,t}^{RE} \right] \\ \left[\eta + \left(1 + \widetilde{\theta}_{t,t-J} \right) \gamma \right] \widehat{h}_{i,t}^{\theta} &= (1 + \widetilde{\theta}_{t,t-J}) (1-\gamma) \left[\rho_A A_t + (1-\tau) s_{i,t} \right] \\ &- \widetilde{\theta}_{t,t-J} \left(1 - \gamma \right) \rho_A^{J+1} A_{t-J} + \widetilde{\theta}_{t,t-J} \gamma \varepsilon \rho_A^{J+1} A_{t-J} \\ \widehat{h}_{i,t}^{\theta} &= \frac{\left(1 + \widetilde{\theta}_{t,t-J} \right) (1-\gamma)}{\eta + \left(1 + \widetilde{\theta}_{t,t-J} \right) \gamma} \rho_A A_t + \frac{\left(1 + \widetilde{\theta}_{t,t-J} \right) (1-\gamma)}{\eta + \left(1 + \widetilde{\theta}_{t,t-J} \right) \gamma} (1-\tau) s_{i,t} \\ &- \frac{\widetilde{\theta}_{t,t-J} \eta}{\eta + \left(1 + \widetilde{\theta}_{t,t-J} \right) \gamma} \left[\frac{1-\gamma}{\eta + \gamma} \right] \rho_A^{J+1} A_{t-J}, \end{split}$$

where the effective diagnosticity parameter $\widetilde{\theta}_{t,t-J}$ is given by (35).

Consider $R_{t+1|t,t-J}$:

$$R_{t+1|t,t-J} = \frac{\mathbb{V}_{i,t} \left(-\gamma \widehat{c}_{i,t+1}^{RE} + A_{t+1} + (1-\tau)a_{i,t+1} \right)}{\mathbb{V}_{i,t-J} \left(-\gamma \widehat{c}_{i,t+1}^{RE} + A_{t+1} + (1-\tau)a_{i,t+1} \right)}$$

$$= \frac{\mathbb{V}_{i,t} \left(-\gamma \left(A_{t+1} + (1-\tau)a_{i,t+1} + \widehat{h}_{i,t}^{\theta} \right) + A_{t+1} + (1-\tau)a_{i,t+1} \right)}{\mathbb{V}_{i,t-J} \left(-\gamma \left(A_{t+1} + (1-\tau)a_{i,t+1} + \widehat{h}_{i,t}^{RE} \right) + A_{t+1} + (1-\tau)a_{i,t+1} \right)}$$

$$= \frac{\mathbb{V}_{i,t} \left((1-\gamma) \left(A_{t+1} + (1-\tau)a_{i,t+1} \right) - \gamma \widehat{h}_{i,t}^{\theta} \right)}{\mathbb{V}_{i,t-J} \left((1-\gamma) \left(A_{t+1} + (1-\tau)a_{i,t+1} \right) - \gamma \widehat{h}_{i,t}^{RE} \right)}$$

where the numerator is

$$V_{i,t} \left((1 - \gamma) \left[\rho_A A_t + u_{A,t+1} + (1 - \tau) s_{i,t} + (1 - \tau) u_{a,i,t+1} \right] - \gamma \widehat{h}_{i,t}^{\theta} \right)$$

$$= (1 - \gamma)^2 \left(\sigma_A^2 + (1 - \tau)^2 \sigma_{a,t}^2 \right),$$

which is increasing in $\sigma_{a,t}^2$ but also a change in $\sigma_{a,t}^2$ have a smaller impact when the progressivity τ is higher. Thus a higher τ is associated with a smaller increase in $R_{t+1|t,t-J}$ and $\widetilde{\theta}_{t,t-J}$.

B Upper bound on DE distortion

Suppose that we are interested in imposing an upper bound on the Smooth DE distortion. Imposing such upper bound on the overreaction in the mean guarantees that both distortions remain finite and non-decreasing as the ratio $R_{t+h|t,t-J}$ goes to infinity. Thus, we propose the following approach.

Let $\overline{\widetilde{\theta}}$ be the desired upper bound of effective overreaction in conditional mean. By effective overreaction we refer to the object defined in equation (10). As a first step, we exploit the fact that the size of the distortion is increasing in $R_{t+h|t,t-J}$ to find the threshold value \overline{R} , such that, for a given θ , for each $R_{t+h|t,t-J} > \overline{R}$, the overreaction in the mean would be larger than $\overline{\widetilde{\theta}}$:

$$\frac{\overline{R}\theta}{1+\theta\left(1-\overline{R}\right)} = \overline{\widetilde{\theta}}$$

It follows that the upper threshold in terms of $R_{t+h|t,t-J}$ is

$$\overline{R} = \frac{\overline{\widetilde{\theta}}}{1 + \overline{\widetilde{\theta}}} \frac{1 + \theta}{\theta}$$

Whenever $R_{t+h|t,t-J} > \overline{R}$, we thus replace θ with θ_R , the value of θ such that the overreaction in the mean is equal to $\overline{\widetilde{\theta}}$. Thus, we solve:

$$\frac{R_{t+h|t,t-J}\theta_R}{1+\theta_R\left(1-R_{t+h|t,t-J}\right)} = \overline{\widetilde{\theta}}$$

and obtain:

$$\theta_{R} = \frac{\overline{\widetilde{\theta}}}{R_{t+h|t,t-J} - \overline{\widetilde{\theta}} \left(1 - R_{t+h|t,t-J}\right)}$$

Plugging in θ_R in the formulas for the overreaction in mean and variance, we obtain:

$$\mathbb{E}_{t}^{\theta}(x_{t+h}) = \mu_{t+h|t} + \theta_{R} \frac{R_{t+h|t,t-J}}{1 + \theta_{R} (1 - R_{t+h|t,t-J})} (\mu_{t+h|t} - \mu_{t+h|t-J})$$

$$\mathbb{E}_{t}^{\theta}(x_{t+h}) = \mu_{t+h|t} + \overline{\widetilde{\theta}} (\mu_{t+h|t} - \mu_{t+h|t-J})$$

and

$$\mathbb{V}_{t}^{\theta}(x_{t+h}) = \frac{1}{1 + \theta_{R} \left(1 - R_{t+h|t,t-J}\right)} \sigma_{t+h|t}^{2}$$

$$\mathbb{V}_{t}^{\theta}(x_{t+h}) = \left[1 + \overline{\widetilde{\theta}} \left(1 - \frac{1}{R_{t+h|t,t-J}}\right)\right] \sigma_{t+h|t}^{2}$$

Note that while the overreaction in the mean remains constant once $R_{t+h|t,t-J} > \overline{R}$, the overreaction in the variance keeps growing as relative uncertainty increases, but it converges to a finite value:

$$\lim_{R_{t+h|t,t-J}\to\infty} \mathbb{V}_{t}^{\theta}\left(x_{t+h}\right) = \left[1 + \overline{\widetilde{\theta}}\right] \sigma_{t+h|t}^{2}$$